Wiley
International Journal of Energy Research
Volume 2024, Article ID 7407501, 25 pages
https://doi.org/10.1155/2024/7407501

WILEY

Research Article

Vigna mungo (L.) Hepper as Heterogeneous Catalyst for Generation of Biodiesel from a Mixture of Multiple Oil Feedstocks

Sujata Brahma,[1] **Bidangshri Basumatary**,[1] **Bikash Chandra Mushahary**,[2] **Siri Fung Basumatary**,[1] **Bipul Das**,[3] **Manickam Selvaraj**,[4] **and Sanjay Basumatary**[1]

[1]*Department of Chemistry, Bodoland University, Kokrajhar 783370, Assam, India*
[2]*Department of Chemical Sciences, Tezpur University, Tezpur, Napaam 784028, Assam, India*
[3]*Chemical Engineering Division, CSIR-North East Institute of Science and Technology, Jorhat 785006, Assam, India*
[4]*Department of Chemistry, Faculty of Science, King Khalid University, Abha 61413, Saudi Arabia*

Correspondence should be addressed to Sanjay Basumatary; waytosanjay12@gmail.com

Received 21 September 2023; Revised 20 April 2024; Accepted 2 May 2024; Published 25 May 2024

Academic Editor: Olubayo Babatunde

A cost-effective catalyst is essential to reduce the expenses of producing biodiesel. This study is aimed at utilizing the waste of the black gram (*Vigna mungo* (L.) Hepper) plant as an efficient catalyst for producing biodiesel from a blend of different edible and inedible oils. The catalyst was developed by igniting the dried material and then subjecting it to calcination at 550°C for 2 h. The feedstock was prepared by mixing the oils in an equivalent ratio for the reaction. Various sophisticated techniques such as XRD, FT-IR, XPS, BET, FESEM-EDX, HRTEM, and SAED were employed to characterize the prepared catalyst. The catalyst's catalytic activity was assessed by transesterification of the oil mixture. The optimized transesterification conditions were 10 wt% of catalyst loading, 9 : 1 of MTOR, 65°C of reaction temperature, and 1.6 ± 0.14 h of reaction time producing 94.79 ± 0.27% of biodiesel yield and 96.86% oil conversion. The calcined catalyst's alkaline solubility was found to be 2.77 mmol/g, basicity as 0.13 mmol/g, and 14.57 per hour as the turnover frequency (TOF). Catalyst reusability was conducted and found that the catalyst could be reprocessed up to three successive cycles. The synthesized biodiesel's physicochemical characteristics were assessed and found to conform to ASTM D6751 and EN 14214 requirements.

1. Introduction

Continuous high energy demand is an outcome of upsurging growth in population, change in lifestyle, industrialization, and urbanization. As a consequence, severe depletion of fossil fuel reserves could be seen with an increase in global warming, high oil prices, etc. [1]. As per the IPCC (Intergovernmental Panel on Climate Change) 2021 report, a 1.5°C rise in surface temperature is estimated for 2021-2040 in comparison to the pre-industrial era [2]. Despite posing serious environmental risks, fossil fuels are the primary source of energy and are predicted to run out by 2050 [3]. Thereafter, the cause emphasizes the need for an alternative that is renewable, cost-efficient, and sustainable that can eventually divert the dependence on fossil fuel reserves.

One such is biodiesel, a mixture of fatty acid methyl ester (FAME), which shows better chemical and physical properties than conventional diesel. Biodiesel is biodegradable, renewable, and nontoxic; has a low sulfur content; emits fewer greenhouse gases; and is easy to handle and transport. It is either used as an individual fuel, mixed with diesel, or blended with diesel and solvent, where the resultant fuels are reported to improve mechanical efficiencies [4]. Veza et al. [5] investigated the effect of palm oil-biodiesel blend and observed an increase in density and kinematic viscosity with increasing the biodiesel percentage.

Biodiesel is synthesized by the most common method called transesterification, which involves the reaction of oil feedstock with alcohols in the presence of an appropriate catalyst. As feedstock, edible oils (for instance, sunflower

oil, soybean oil, palm oil, and rapeseed oil) are the major attraction for biodiesel synthesis [6]. Edible oils are extensively produced by countries like Brazil, China, India, France, the United States, and Canada. During 2020-2021, the production of edible oils touched up to 210 million metric tons worldwide [7]. Since edible oils are necessary to meet the food requirement, the reliance on them for the manufacture of biodiesel is limited. Their extensive use results in a hike in food demand and in its price, which forbids their usage as a source for biodiesel synthesis. Another emerging feedstock is inedible oils, which are unsuitable for human uptake and cheap; hence, they are regarded as a suitable source to produce biodiesel. Inedible oils (karanja, neem, jatropha, mahua, etc.) are low in price and require nonfertile land for cultivation, but the increased demand for nonedible oils may rise in the clearing of forest areas for the cultivation of such crops. Other drawbacks of nonedible oils are their high acid value, and their requirement in the cosmetic, biolubricant, and soap industries, which may shorten the availability of nonedible oils [8].

In addition, tons of frying oils are discarded after use (called WCO, waste cooking oil), which has drawn the attention of researchers for biodiesel synthesis. However, utilization of WCO requires additional processing costs for purification from impurities and esterification before carrying out transesterification reactions [9]. Furthermore, algal feedstocks are also utilized by various researchers as feedstock for biodiesel production but are subject to many disadvantages, such as their production and extraction challenges that require huge investment [10]. Additionally, waste animal fats, the by-products derived from animal meat processing and rendering plants, also serve as promising feedstock for biodiesel production. Although their use can lessen the waste produced by slaughterhouses, it will cost more money and energy because of the high concentration of FFAs and water they contain. This can lead to low yields and make separation and purification more difficult. It has been mentioned by Toldrá-Reig et al. [11] that the refining of crude biodiesel derived from animal fats and vegetable oil is more expensive than the latter.

Single oil feedstock (either edible or nonedible) is widely employed, but the usage of single raw materials accounts for many issues, such as the availability of raw materials and the extensive requirement for cultivable land. Production of biodiesel from single feedstocks faces issues during esterification and transesterification [10]. In this view, the blending of different types of oils has drawn the attention of the scientific community. Blending different oils with different (either high or low) FFA can result in a feedstock with reduced FFA, making it suitable for biodiesel production. The mixing of multiple feedstocks also reduces the dependency on the availability of a particular feedstock. Thus, mixing can eliminate the time and cost required for esterification of the feedstock before transesterification [10]. Also, Kusumo et al. [12] mentioned that the physiochemical properties of biodiesel might be improved by using a multifeedstock. In this regard, various studies have been carried out utilizing different blends of feedstock, such as mixture of *Sterculia foetida* and rice bran oil [12]; mixed castor and soybean oils [13]; blend of hazelnut and sunflower oil [14]; combination of waste fish, bitter almond, and waste cooking oil [15]; and mixed *Jatropha curcas* and *Ceiba pentandra* [16].

The catalytic transesterification method proceeds with the aid of homogeneous, heterogeneous, and enzyme-based catalysts. The homogeneous-based transesterification reaction results in high biodiesel conversion in a short reaction time but corresponds to saponification, difficulties in separation, high energy consumption, and large wastewater generation [1]. Whereas, the enzyme catalysts that are insensitive to FFAs produce high biodiesel conversion, but their production requires high capital investment as well as a longer reaction time for biodiesel conversion [17]. NaOH, KOH, H_2SO_4, CH_3OK and CH_3ONa [18], *Clostridium* sp. [19], *C. antarctica* lipase B [20], *Thermomyces lanuginosus* [21], etc. are some of the reported homogeneous and enzyme catalysts employed by various researchers to produce biodiesel. Lastly, heterogeneous catalyst-mediated transesterification proceeds in milder reaction conditions with easy separation and reusability and, thus, is regarded as the most efficient catalyst in biodiesel synthesis. Selemani and Kombe [22] also mentioned that heterogeneous catalysts could reduce high FFA in a short period of time. Some heterogeneous catalysts reported are lithium-based chicken bone [23], KNO_3-impregnated oil shale ash [24], ZIF-8 MOF-derived CaO/ZnO catalyst [25], CaO [26], etc.

The cost of feedstock and catalyst severely affects biodiesel production on a commercial scale [27]. To reduce the expenses of biodiesel production, catalysts derived from agricultural leftover materials as heterogeneous catalysts are seen to rise rapidly. Agricultural waste-derived catalysts are abundant in nature, low-cost, and show high catalytic efficiency because of the abundance of alkali and alkaline earth metals existing as carbonates and oxides [9]. Various agrowaste-based catalysts have been noticed from the works done by using elephant ear pod husk [28], *Citrullus lanatus* and *Musa acuminate* peels [29], *L. perpusilla* Torrey ash [30], waste banana peels [31], moringa leaves [32], *Musa acuminata* peduncle [33], *Musa acuminata* peel [3], Kola nut pod husk [34], *Citrus sinensis* peel [35], *Brassica nigra* [36], banana peel-supported sulfonic acid [37], *M. champa* peduncle [38], blend of coca, kola nut, and fluted pumpkin husks [39], blend of plantain peels [40], H_2SO_4/KOH-doped *Delonix regia* char [41], Li-incorporated arecanut husk ash [42], sugarcane bagasse [43], potato peel [44], *Xanthium strumarium* seed shells [45], and many more.

Black gram (*Vigna mungo* (L.) Hepper) is a leguminous plant that belongs to the Fabaceae family, originated from South Asia, and is distributed among the subtropical and tropical parts of India [46, 47]. It is an erect and fast-growing crop whose height reaches 30-100 cm [48]. Black gram is a good source of proteins (mainly globulins), fibres, carbohydrates, and fats. India leads the world black gram production, accounting for over 70% of global output, with Myanmar and Pakistan following closely behind [49]. Black gram is cultivated during the kharif season. After the maturation of the pods, the crop is stacked and allowed to dry. On drying, the seeds are separated from the pods. In most parts of the world, the leftover plants are discarded as waste,

which can account for intense environmental pollution. Developing this unhandled agricultural waste as a catalyst is one of the potential ways to tackle this environmental issue. It is widely reported that agricultural wastes are advantageous as catalysts because they contain plenty of alkali and alkaline earth metals which make them suitable catalysts for biodiesel synthesis [50]. Furthermore, utilizing such waste as a catalyst for biodiesel production can cut down on the cost associated with the preparation of catalyst.

Nowadays, the use of various process intensification techniques is being reported by various researchers. These technologies improve biodiesel production efficiency and decrease reaction time, which overcomes the drawbacks of conventional methods [51]. These techniques include microwave-irradiation and ultrasonication [51, 52]. In a study of microwave-assisted transesterification of the combination of honne, rubber seed, and neem oils, 98.45 wt% of biodiesel yield was reported within 6 min under microwave heating of 150 W, as reported by Falowo et al. [53]. An innovative approach utilizing the combination of microwave and ultrasonication methods to analyze biodiesel production from a blend of *Ricinus communis* oil and used cottonseed cooking oil was carried out by Kodgire et al. [51]. The study resulted in $92.11 \pm 0.06\%$ of biodiesel yield with improved physicochemical properties in 12.3 min. In addition, machine learning algorithms like artificial neural network, response surface methodology, linear regression, extreme learning machine (ELM), cuckoo search (CS), and genetic algorithms are trending among academics. These algorithms have a tendency to enhance biodiesel productivity and economic feasibility [10, 54]. Mujtaba et al. [52] used ultrasonic assistance to transesterify a combination of palm and sesame oil. They used CS optimization algorithm in conjunction with ELM in their investigation, yielding 95.89% biodiesel.

Further, the physicochemical characteristics of biodiesel are claimed to be improved by the use of additives. However, at low dosages, their impact on low-temperature performance is minimal. For instance, fractionation technologies such as distillation and winterization are stated to provide better improvements in low-temperature performance. An extraordinary approach of urea inclusion in order to remove saturated fatty acid methyl esters was undertaken by Liu and Tao [55] which resulted in a biodiesel with reduced cloud point. In another study, Yeong et al. [56] utilized the vacuum distillation technique to improve the cold flow characteristics of biodiesel synthesized from palm fatty acid distillate.

A literature survey depicting the biodiesel production from various single or blended feedstocks utilizing various kinds of heterogeneous catalysts is listed in Table 1. This literature survey suggests that the adaptation of blended or mixtures of oils as biodiesel feedstock catalysed by heterogeneous ash-based catalyst is limited in this area. Also, it has been noticed that the leftover parts of black gram have not been explored as a heterogeneous catalyst as well as its catalytic activity for biodiesel production till date. The waste of black gram has the capability to be employed for catalyst production, as it is cultivated in several countries, and the leftovers are discarded as waste. As a result, it is inexpensive, widely available, easily separated, and reusable without requiring any additional modification. Hence, in this study, the waste part of the black gram plant is applied as a heterogeneous catalyst to facilitate the transesterification of a feedstock prepared from the mixing of five different types of oils for the first time.

2. Material and Method

2.1. Materials. The postharvested plant residue of black gram, *Vigna mungo* (L.) Hepper, was collected from Runikhata of Chirang district (located at 26.6342° N, 90.3819° E), Assam, India, during the month of February for catalyst preparation. Five different types of oils were used as feedstock for biodiesel production. Edible oils, *viz*., soybean, sunflower, and canola oil, utilized in this experiment were bought from the local store in Kokrajhar town, while the other two inedible oils, *viz*., pongamia and jatropha oil, were purchased from Harvi Trading Company (Rajasthan).

The chemicals and solvents like methanol (≥99.0%), anhydrous sodium sulfate (≥99.0%), petroleum benzine (60-80°C), acetone (99%), ethyl acetate (≥99.5%), aniline, phenolphthalein, and bromothymol blue were purchased from Merck Company. Benzoic acid and 4-nitroaniline were purchased from Avantor Performance Materials India Limited and Loba Chemie (Mumbai, India), respectively. Nile blue and silica gel G for TLC were purchased from SISCO Research Laboratories (Mumbai, India).

2.2. Catalyst Preparation. The plant of *Vigna mungo* was dried for 15 days under sunlight. After which, the waste part was burned into ash in the open air, which was later calcined at 550°C for 2 h in a programmable muffle furnace and stored in the desiccator. Then, using a mortar and pestle, the burnt ash was ground into fine particles (Figure 1) and kept in an air-sealed container for later use as a catalyst and characteristic analysis.

2.3. Characterization of the Catalysts. The presence of different functional groups in the uncalcined catalyst as well as the calcined catalyst was examined using an FT-IR spectrometer (Shimadzu IRAffinity-1S) in the wavenumber range of 4000-500 per cm. The chemical components present in the catalysts were investigated using a powder XRD pattern (Xpert'3 pro). The catalyst's surface area, pore diameter, and pore volume were assessed from the BET (Brunauer-Emmett-Teller) method, BJH (Barrett-Joyner-Halenda) model, and adsorption-desorption isotherm under N_2 adsorption at 77 K using the surface area analyzer Quantachrome (3.0 ASiQwin™). The surface morphology of the catalyst was studied by FESEM (Carl Zeiss NTS GmbH, Oberkochen, Germany) analysis, and the quantitative analysis of the elements was investigated from EDX data. The HRTEM analysis as well as the SAED pattern was carried out utilizing JEOL (JEM-2100, 200 kV) to inspect the structural information of the catalyst. X-ray photoelectron spectrometer (XPS) (ESCALAB Xi+, USA) was used to evaluate the catalyst's composition. The soluble alkalinity, basicity, and pH values of the calcined catalyst were calculated by following the methods reported in the literature [57].

Table 1: Recent works reported on biodiesel production using various heterogeneous catalysts.

Feedstock	Catalyst	Reaction conditions (MTOR; catalyst loading; temperature; time)	Biodiesel, (Y) yield or (C) conversion (%)	References
Clarias gariepinus–Nicotiana tabacum–Elaeis guineensis	CaO derived from agricultural waste	4.15 : 1; 5 wt%; 79.68°C; 79.79 min	99.19 (Y)	Adepoju et al. [26]
Rubber oil–neem oil	Elephant ear pod husk	11.44 : 1; 2.96 wt%; 150 W, 5.88 min	98.77 (Y)	Falowo et al. [28]
Cucurbita pepo oil–*Chrysophyllum albidum* oil–Papaya seed oil	*Citrullus lanatus* and *Musa acuminate* peels	6.97 : 1; 5 wt%; 80°C; 70 min	98.00 (Y)	Adepoju et al. [29]
Yellow oleander oil–rubber seed oil	Cocoa, kola nut, and fluted pumpkin husks	9 : 1; 1.5 wt%; 55°C; 40 min	95.02 (Y)	Falowo and Betiku [39]
Ricinus communis oil–used cottonseed cooking oil	CaO	9.7 : 1; 2.8 wt%; 12.3 min	92.19 (Y)	Kodgire et al. [51]
Soybean oil–sunflower oil–canola oil–jatropha oil–pongamia oil	*M. chinensis*	9 : 1; 5 wt%; 65°C; 11 min	95.82 (Y)	Brahma et al. [17]
Waste cooking oil–refined palm oil	Fly ash	13.57 : 1; 6.7 wt%; 55°C; 120 min	73.8 (Y)	Vargas et al. [92]
Linseed–marula seed oil	Eggshells/banana peels	15 : 1; 3.5 wt%; 65°C; 60 min	95.03 (Y)	Etim et al. [81]
WCO–waste palm oil–waste animal fat	Waste marble tiles and plantain peduncle	6.01 : 1; 2 wt%; 61°C; 149.98 min	98.31 (Y)	Amenaghawon et al. [93]
Waste edible oils	$CoFe_2O_4$/GO/SrO	16.3 : 1; 5%; 69°C; 53.76 min	98.63 (Y)	Zou et al. [94]
Soybean oil	*Pouteria sapota*	6 : 1; 3 wt%; 65°C; 120 min	92 (Y)	Aleman-Ramirez et al. [95]
Sunflower oil	*Pouteria sapota*	9 : 1; 5 wt%; 65°C; 120 min	92 (Y)	Aleman-Ramirez et al. [95]
Soybean oil	*Parkia speciosa*	15 : 1; 5 wt%; 40°C; 180 min	96.4 (Y)	Sarkar et al. [96]
Soybean oil	Eggshell–moringa leaves	12 : 1; 2%; 65°C; 78 min	94.44 (Y)	Aleman-Ramirez et al. [97]
Soybean oil	SrO–ZnO/MOF	11 : 1; 5 wt%; 80°C; 5 min	99.5 (Y)	Yang et al. [98]
Palm oil	Durian peel	15 : 1; 5 wt%; room temperature; 10 min	97.4 ± 0.3 (C)	Sitepu et al. [99]
WCO	Cat.TS–7 based on natural zeolite	9 : 1; 1.5 wt%; 60°C; 120 min	93 (Y)	Saad et al. [100]
WCO	MCNT@CdO	10 : 1; 10%; 120°C; 180 min	92.3 (Y)	Ahranjani et al. [101]

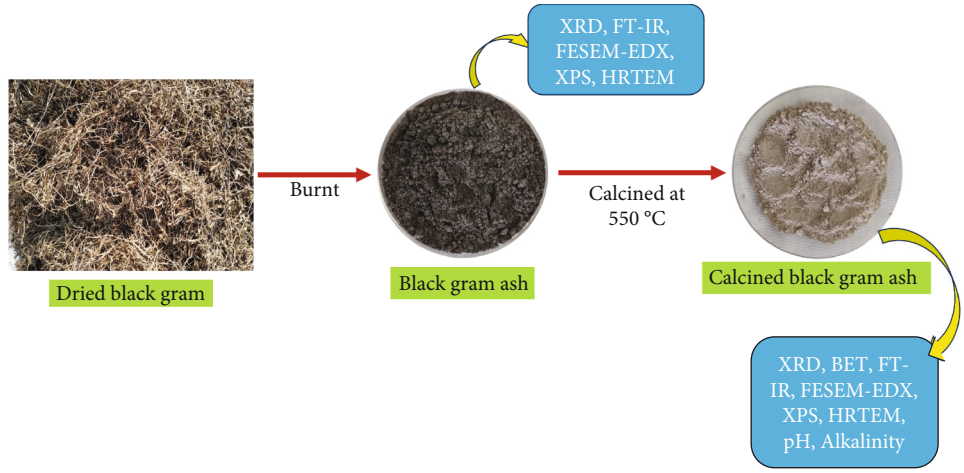

Figure 1: Schematic diagram of preparation of *Vigna mungo* catalyst.

2.4. Feedstock Preparation. For this study, the feedstock utilized for biodiesel production was prepared by mixing the five different oils in an equivalent ratio (1 : 1 : 1 : 1:1) in a similar manner as the previous study [17]. The equivalent mixture was taken in a 250 mL beaker and stirred in a magnetic stirrer set at 650 rpm for 30 min at room temperature (32°C) to form a homogeneous oil mixture. The homogeneous oil mixture was then utilized as a feedstock for this study.

2.5. Transesterification of the Homogeneous Oil Mixture with Methanol. In this study, the transesterification of the oil mixture was performed by taking a homogeneous oil mixture of 2 g in a two-neck round-bottomed flask of 100 mL fitted with a water condenser on a hot plate magnetic stirrer. The different reaction conditions like catalyst loading, methanol-to-oil molar ratio (MTOR), and reaction temperature were varied from 5–15 wt%, 3 : 1–12 : 1, and 35–75°C, respectively, and were inspected to find the optimum reaction parameters. The reflux condenser was used for reaction temperatures beyond 60°C; in addition, the stirring speed of the magnetic stirrer was set to 650 rpm for all the experiments. The completion of the reaction was confirmed by TLC, and the time was recorded. After the reaction was finished, the mixture was allowed to settle in a separating funnel. Two separate layers of biodiesel were then generated by shaking the mixture and extracting the biodiesel with petroleum ether. The lower layer was removed, while the top layer (biodiesel) was collected. The extraction process was continued four to five times and stored overnight by adding anhydrous Na_2SO_4. After filtering the extracted solution, the solvent was removed using a vacuum rotary evaporator (QuickVap, Almicro) set at 50°C to obtain biodiesel. The biodiesel yield (%) obtained was determined as per equation (1) mentioned by Aleman-Ramirez et al. [32].

$$\text{Biodiesel yield}\,(\%) = \frac{\text{Amount of biodiesel obtained}}{\text{Amount of oil taken}} \times 100. \quad (1)$$

The optimization of reaction parameters was performed in triplicate, and the results are represented as mean ± standard deviation.

2.6. Characteristic Study of Produced Biodiesel. The variation of absorption bands in the oil feedstock and the synthesized biodiesel was investigated using FT-IR spectrometer (Shimadzu, MIRacle 10), where the IR spectra were recorded in 4000 to 500 per cm of the wavenumber range. The ^{1}H NMR of the oil and biodiesel was characterized by NMR spectrometer (BRUKER AVANCE II, 400MHz) using deuterated chloroform ($CDCl_3$) as the solvent. Various compositions of the biodiesel were studied using GCMS spectrometer (PerkinElmer Clarus680 GC/600C MS). At first, the temperature was regulated to 60°C for 6 min. Later, the temperature was raised to 180°C at 5°C/min, and then, at a rate of 10°C/min, the temperature was elevated to 280°C. The sample was subjected to the spectrometer when the temperature was set to 250°C and examined using TurboMass Ver5.4.2 software. The carrier gas (helium) was split in a ratio of 20 : 1 at 1 mL/min of the flow rate. The biodiesel's fuel characteristics like density, kinematic viscosity, cetane index, American petroleum index (API), diesel index, iodine value (IV), saponification number, aniline point, and higher heating value (HHV) were evaluated from the standard equation, and the standard criteria are established in Table 2 [58, 59]. Thereafter, ^{1}H NMR data was used to estimate the percentage of oil conversion using equation (2).

$$\text{Oil conversion}\,(\%) = \frac{(2 \times X_{\text{Me}})}{(3 \times X_{\text{CH}_2})} \times 100. \quad (2)$$

Here, X_{Me} and X_{CH_2} are integral areas of the methoxy protons and methylene protons, respectively [4].

3. Results and Discussion

3.1. Characterization of Black Gram (Vigna mungo (L.) Hepper) Catalyst

3.1.1. Powder X-Ray Diffraction Analysis. An XRD study was conducted to investigate the crystalline chemical components present in the uncalcined, calcined, and 3rd recycled catalysts, which are illustrated in Figure 2. The results were analyzed with the help of JCPDS along with reported

Table 2: Standard criteria of physicochemical parameter.

Physicochemical property	Standard equations	Standard criteria	Reference
Cetane index	$46.3 + \frac{5458}{\text{Saponification value}} - 0.225 \times \text{iodine value}$	ASTM D2015	Adepoju et al. [58]
API	$\frac{141.5}{\text{Specific gravity@15°C}} - 131.5$	ASTM D2015	Adepoju et al. [58]
HHV (MJ/Kg)	49.43 – [0.041(saponification value) + 0.015 (Iodine value)]	ASTM D2015	Adepoju et al. [58]
Diesel index	$\frac{\text{Cetane index} - 10}{0.72}$	ASTM D2015	Adepoju et al. [58]
Aniline point (°F)	$\frac{\text{Diesel index} \times 100}{\text{API}}$	ASTM D2015	Adepoju et al. [58]
Iodine value (IV)	$\sum$(254 × number of double bonds × composition percentage of each fatty acid)/molecular weight of each fatty acid	Empirical method	Basumatary et al. [59]
Saponification number (mg KOH/g of oil)	$\sum$(560 × composition percentage of each fatty acid)/molecular weight of each fatty acid	Empirical method	Basumatary et al. [59]

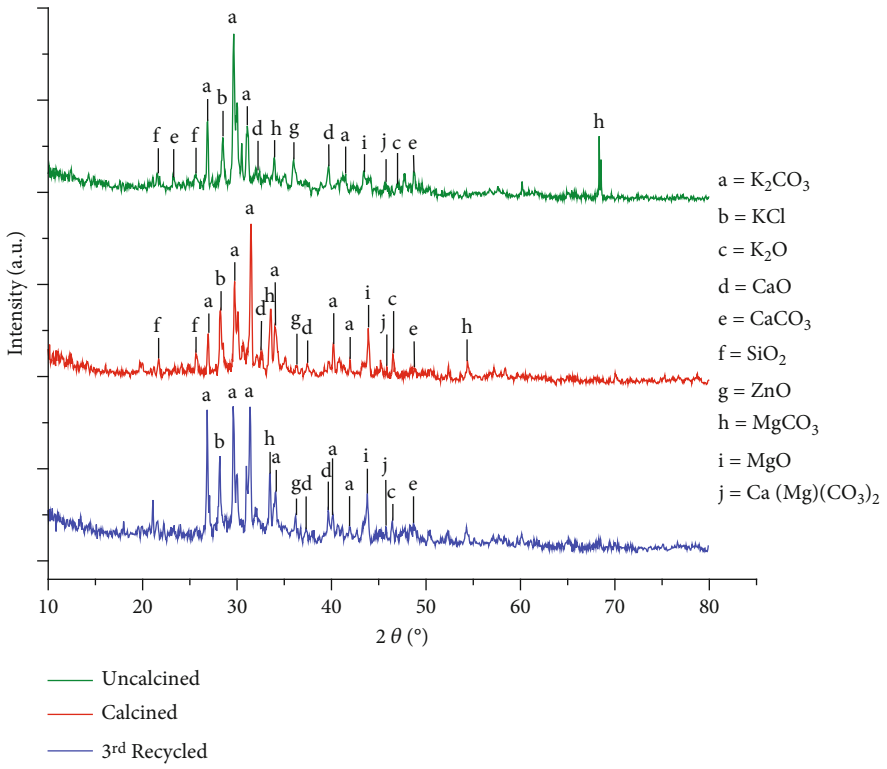

Figure 2: XRD patterns of uncalcined, calcined, and 3rd recycled catalysts.

literature where the presence of K_2CO_3, K_2O, CaO, $CaCO_3$, KCl, SiO_2, etc. is revealed in the present catalysts. The presence of K as carbonates in the catalysts was indicated by the high-intensity peaks observed at 2θ values of 26.83, 29.57, and 41.58 for uncalcined catalyst; 29.75, 26.86, 40.45, and 41.90 for calcined, and 26.83, 29.58, 34.08, 40.26, and 41.90 for the 3rd recycled catalyst [45]. Whereas, peaks at 2θ values of 46.71 (uncalcined), 46.60 (calcined), and 46.60 (3rd recycled) illustrated the presence of K in the form of K_2O. These results are in line with the *Brassica nigra* catalyst described by Nath et al. [36] as well as the coconut husk ash catalyst studied by Vadery et al. [60]. The 2θ values observed at 28.47 (for uncalcined catalyst), 28.25 (for calcined catalyst), and 28.25 (for 3rd recycled catalyst) can be ascribed to KCl, and these values agree with the KCl values observed for the mixture of agrowaste catalysts reported by Falowo and Betiku [39]. The occurrence of peaks at 2θ values of 23.20 and 48.73 in the uncalcined catalyst, 48.67 in the calcined catalyst, and 23.28 and 48.73 in the 3rd recycled catalyst are due to the occurrence of $CaCO_3$. This

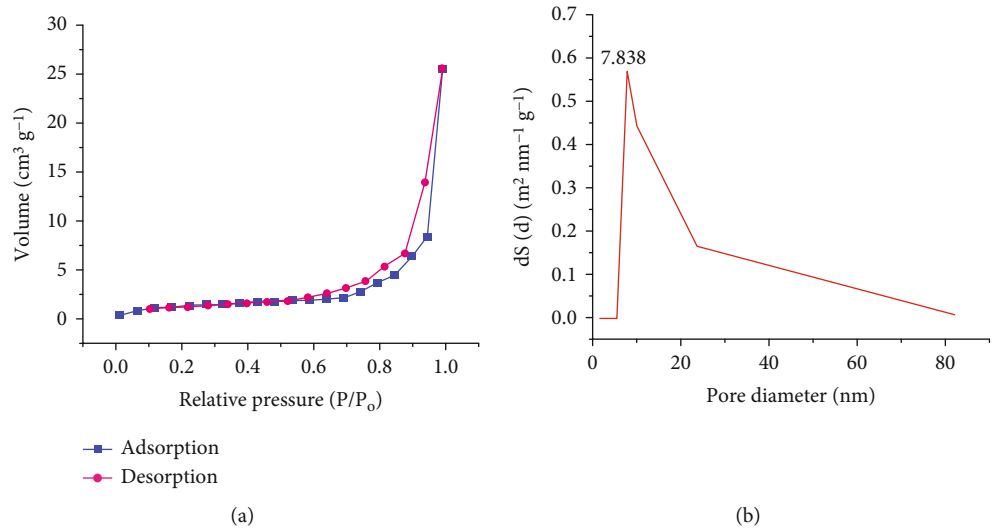

Figure 3: (a) N_2 adsorption-desorption isotherm and (b) adsorption pore-size distribution of calcined catalyst.

data is supported by the XRD data of *sesamum indicium* described by Nath et al. [61]. Further, the peaks for CaO in the catalysts are observed from the 2θ values of 32.16, 39.72, and 43.18 in the uncalcined catalyst; 32.52, 37.42, and 54.19 in the calcined catalyst; and 37.34 and 39.70 in the 3rd recycled catalyst. The results, thus, obtained are like those stated by Gohain et al. [62] and Niju et al. [63]. Furthermore, the peaks observed at the 2θ values at 21.56, 25.58 (uncalcined catalyst), 21.61, 25.61 (calcined catalyst), and 25.73 (3rd recycled catalyst) can be ascribed to SiO_2, and these values are similar to those of the sugarcane bagasse reported by Basumatary et al. [43]. The MgO in these catalysts is described by the 2θ values at 43.64 (uncalcined catalyst), 43.92 (calcined catalyst), and 43.82 (3rd recycled catalyst). Similar 2θ values for Mg as MgO are reported by Nath et al. [38] which were 43.19 and 43.82 for the calcined *M. champa* peduncle and 3rd reused catalysts, respectively. The presence of Mg as $MgCO_3$ is revealed by the 2θ values at 33.82 in the uncalcined catalyst, 33.58 and 54.47 in the calcined catalyst, and 33.46 and 54.41 in the 3rd recycled catalyst. Also, the occurrence of $Ca(Mg)(CO_3)_2$ (dolomite) is visible from the 2θ values for the uncalcined, calcined, and 3rd recycled catalysts at 45.81, 45.87, and 45.81, respectively. Analogous 2θ values for $MgCO_3$ and $Ca(Mg)(CO_3)_2$ are noticeable from the work of Basumatary et al. [50]. Lastly, the peaks for ZnO were identified from the 2θ value of 36.03 in the uncalcined catalyst and 36.19 both in the calcined and 3rd reused catalysts, which coincided with the 2θ values mentioned by Malani et al. [64] and Xie and Huang [65].

3.1.2. Surface Area Analysis. The surface area of *Vigna mungo* (L.) Hepper calcined at 550°C was analyzed. The BET and BJH surface areas were discovered as 7.204 m^2/g and 7.617 m^2/g, respectively. Comparatively, the surface area found in this study is larger than those mentioned in the works of Falowo et al. [28] (1.2960 m^2/g), Adepoju [66, 67] (1.20 m^2/g, 1.10 m^2/g), Betiku et al. [34] (5.2199 m^2/g), and Adepoju et al. [68] (1.30 m^2/g). Thus, the surface area of this current catalyst is significantly higher than that of the cited

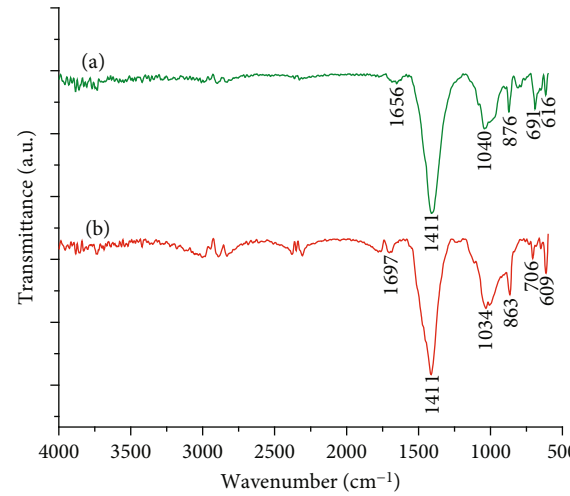

Figure 4: FT-IR spectra of (a) uncalcined and (b) calcined catalysts.

catalysts and, thus, has good catalytic activity. The N_2 physisorption isotherms are shown in Figure 3, which indicates that the catalyst is a type IV isotherm with a hysteresis loop of type H3. This observation reflects that the catalyst is mesoporous in nature [38]. The BJH pore diameter and pore volume were 7.838 nm and 0.045 cm^3/g, respectively. Also, pore size distribution was between 5.4188 nm and 23.5548 nm, which is a characteristic feature of mesoporous material, and this supports the N_2 adsorption-desorption isotherm. This finding is identical to that observed in the study of *Musa acuminata* peel catalyst [4].

3.1.3. Fourier Transform Infrared Spectroscopy Analysis. The FT-IR spectra of the uncalcined and calcined catalysts are depicted in Figure 4. The absorption bands at 1656 and 1697 per cm of uncalcined and calcined catalysts, as well as 1411 per cm in both catalysts, are due to C–O stretching vibrations demonstrating the existence of carbonates in the catalysts [69]. The bands in the region of 1040-1030 per

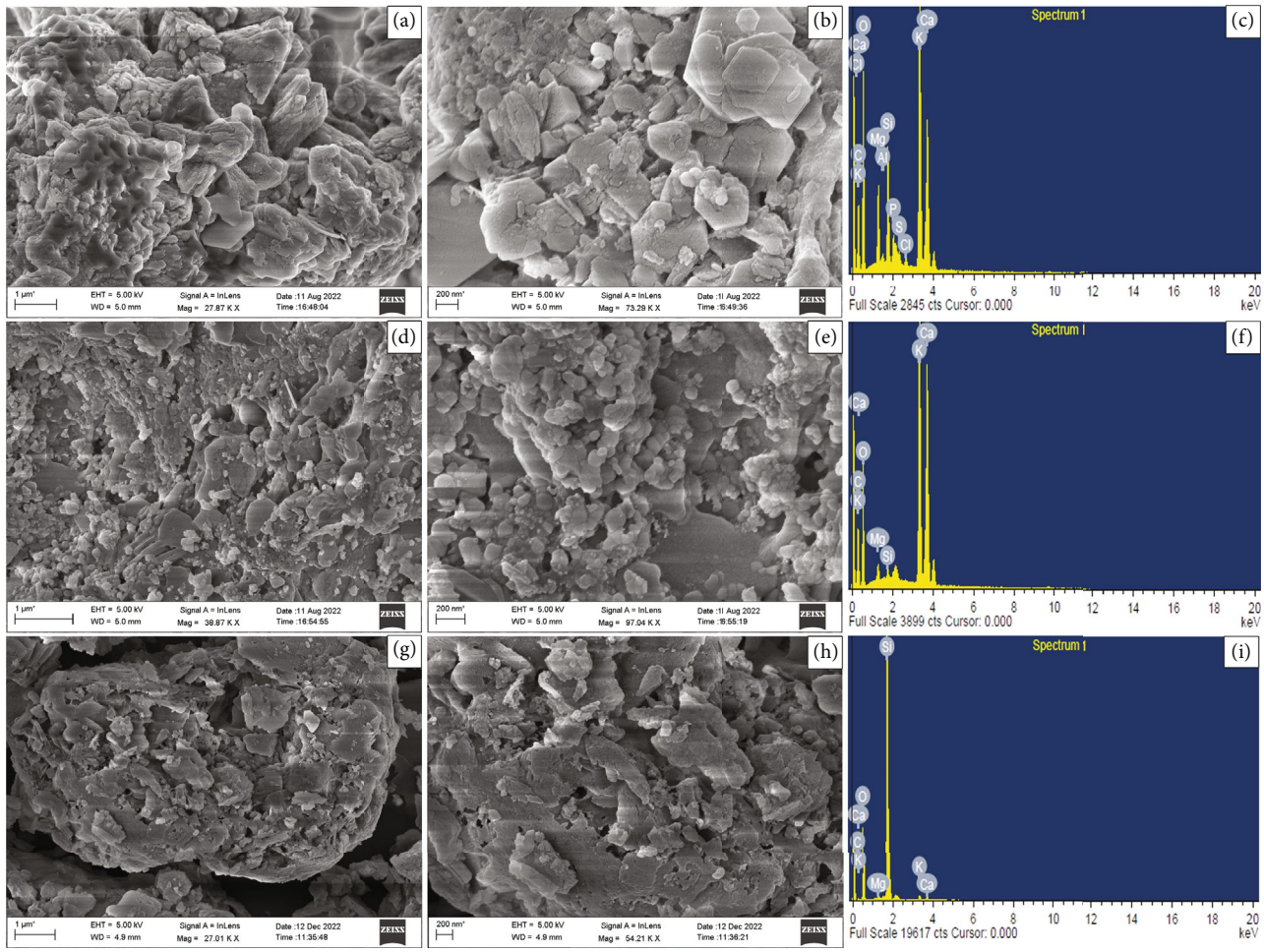

Figure 5: (a, b, d, e, g, h) FESEM images and (c, f, i) EDX patterns of (a, b) uncalcined, (d, e) calcined, and (g, h) 3rd recycled catalysts.

Table 3: FESEM-EDX analyses of *Vigna mungo* catalyst.

Elements	Composition of catalysts					
	Uncalcined		Calcined		3rd recycled	
	Weight %	Atomic %	Weight %	Atomic %	Weight %	Atomic %
C	20.19	29.79	14.20	22.79	6.23	9.96
O	49.46	54.81	48.72	58.70	50.86	61.00
Mg	3.44	2.51	1.08	0.86	0.48	0.38
Si	4.21	2.65	0.62	0.43	40.78	27.86
K	13.47	6.11	17.42	8.59	0.94	0.46
Ca	8.99	3.97	17.96	8.64	0.71	0.34
Al	0.23	0.15	—	—	—	—

cm in the two catalysts are because of Si–O–Si bond vibrations of SiO_2 [57]. The appearance of peaks at 876, 691, and 616 per cm in the uncalcined catalyst as well as peaks at 863, 706, and 609 per cm in the calcined catalyst are due to the stretching vibrations of metal oxides in the catalysts [17]. These findings are in accordance with the outcomes of XRD analysis (Figure 2) that verified the presence of various metals as carbonates and oxides in the catalysts.

3.1.4. Field Emission Scanning Electron Microscopy Analysis. The FESEM analyses of the uncalcined, calcined, and 3rd recycled *Vigna mungo* (L.) Hepper catalyst is depicted in Figure 5. Various distinct morphologies are observed in the data. In the uncalcined catalyst, clusters of several hexagonal, rectangular, and several other polygons are visible, some of which are arranged in sheet-like patterns (Figures 5(a) and 5(b)). In addition, building blocks of some cubic structures

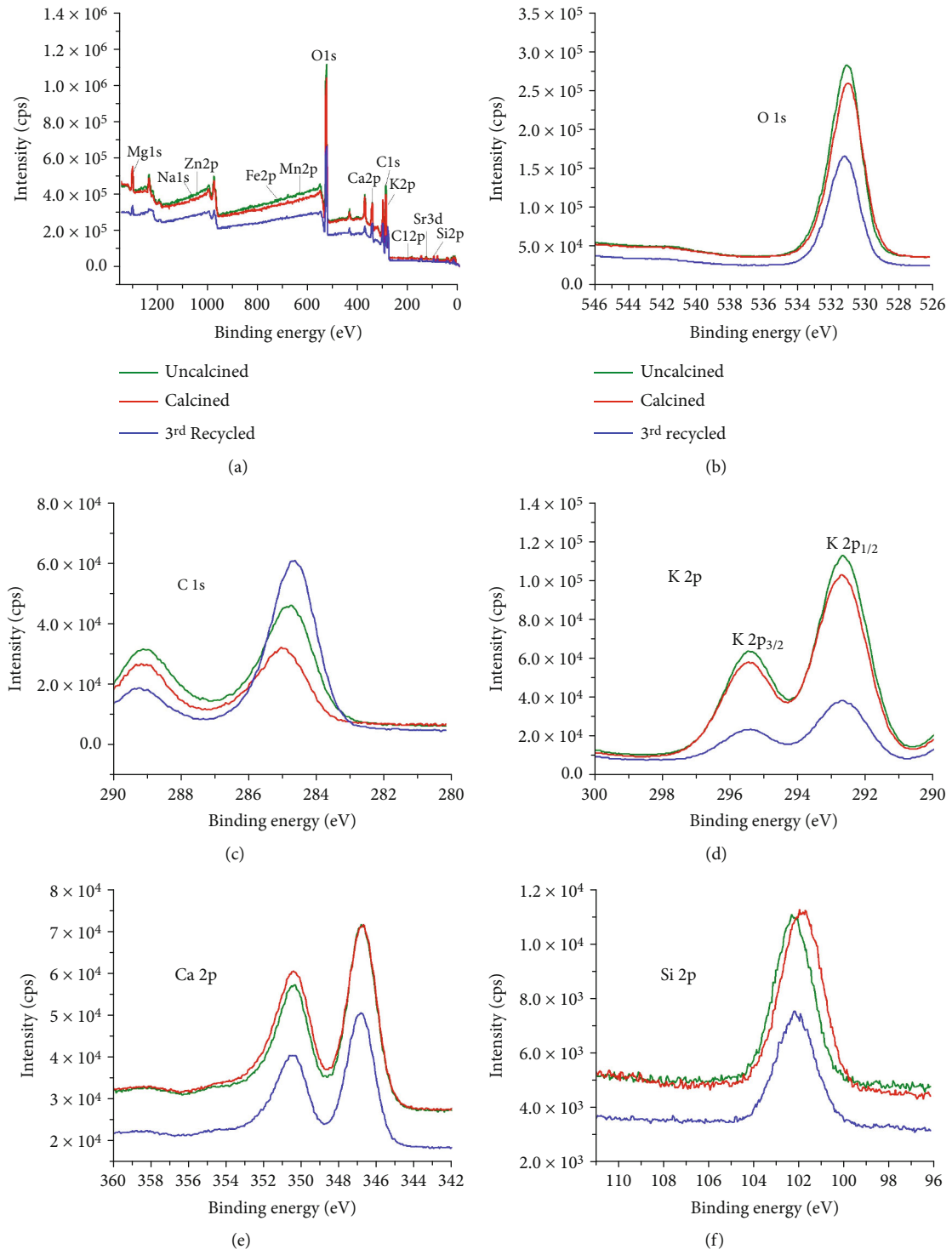

FIGURE 6: (a) XPS survey and XPS patterns of (b) O 1 s, (c) C 1 s, (d) K 2p, (e) Ca 2p, and (f) Si 2p of uncalcined, calcined, and 3rd recycled catalysts.

are also spotted. In the calcined catalyst, the structural morphology is almost similar to that in the uncalcined catalyst. However, much porosity and agglomeration are seen in this catalyst, which may be the cause for its better catalytic efficiency in contrast to the uncalcined catalyst (Figures 5(d) and 5(e)). Further, in the 3rd recycled catalyst, the arrangement of some irregular structures with less porous assembly is seen, which may have wiped out its activity (Figures 5(g) and 5(h)).

The average particle size of uncalcined and calcined catalysts was determined from the FESEM images as 91.658 nm and 121.919 nm, respectively. It is worth mentioning that the

Table 4: XPS analysis of *Vigna mungo* catalyst.

Elements	Composition of catalyst (atomic %)		
	Uncalcined	Calcined	3rd recycled
O 1 s	38	44.16	44.46
K 2p	8.16	9.96	3.98
Cl 2p	0.2	0.27	0.09
Si 2p	2.64	3.71	3.8
Mg 1 s	1.61	3.39	2.46
Na 1 s	0.17	0.15	0.15
C 1 s	48.07	36.57	44.08
Zn 2p	0.1	0.14	0.15
Fe 2p	0.24	0.28	0.25
Mn 2p	0.3	0.18	0.18
Sr 3d	0.2	0.26	0.2
Ca 2p	0.15	0.35	0.2

particle size increased during calcination which is probably because of the sintering effect during catalysts' calcination [70, 71].

The elemental composition of the uncalcined, calcined, and 3rd recycled catalysts was studied with the help of the EDX analysis technique (Figures 5(c), 5(f), and 5(i)). The weight % along with the atomic % of the respective elements are summarized in Table 3. From the analysis, it has been found that the three catalysts consist of C, O, Mg, Si, K, Ca, and Al. Among these, K, Ca, C, and O are present as major elements, while Mg, Si, and Al are present in minor traces. It is notable that K and Ca were observed to have the highest weight % in comparison to other metals. It is seen from Table 3 that the K and Ca content in the uncalcined catalyst was 13.47 wt% and 8.99 wt%, respectively, which was observed to increase during calcination, showing 17.42 wt% and 17.96 wt% of the K and Ca amounts, respectively, in the calcined catalyst. However, a decline in the K and Ca contents was seen in the 3rd recycled catalyst, which could be due to leaching during repetitive use of the catalyst for the transesterification reaction [38]. Also, a considerable amount of O and C is observed in the three catalysts, which suggests that K and Ca in the catalysts are present as metallic carbonates as well as oxides such as K_2CO_3 and K_2O, and likewise $CaCO_3$ and CaO, which are assisted by the XRD and FT-IR data. Changmai et al. [72] specified that the existence of K and Ca in the catalyst shows good catalytic activity for transesterification. Thus, the calcined catalyst showed good catalytic efficiency due to the presence of basic sites, *viz*., K and Ca.

3.1.5. X-Ray Photoelectron Spectroscopy Analysis. The XPS analysis of the catalyst that was conducted to study the surface chemical composition is shown in Figure 6, and the atomic % of the respective element is listed in Table 4. The results of this study displayed the existence of O, K, Cl, Si, Mg, Na, C, Zn, Fe, Mn, Sr, and Ca, which support the data obtained from the EDX study. The surface of the calcined catalyst contained major elements such as oxygen (44.16%), carbon (36.57%), and potassium (9.96%), which are in the form of K_2CO_3 and K_2O, as exposed from the XRD data. In addition, other elements are also observed in small amounts, which are silicone (3.71%), magnesium (3.39%), calcium (0.35%), iron (0.28%), chlorine (0.27%), strontium (0.26%), manganese (0.18%), sodium (0.15%), and zinc (0.14%). From the O 1 s spectra, binding energies of 531.11 eV, 531.01 eV, and 531.19 eV were observed for uncalcined, calcined, and 3rd recycled catalysts, respectively, which resembled the presence of oxygen as oxides in the three catalysts. From the K 2p spectra, two peaks are observed for each catalyst, with binding energies of 295.46 eV and 292.69 eV for the uncalcined catalyst, 295.47 eV and 292.73 eV for the calcined catalyst, and 295.53 eV and 292.69 eV for the 3rd recycled catalyst. In these spectra, the higher and lower peaks of K 2p were designated for K $2p_{1/2}$ and K $2p_{3/2}$, respectively, representing +1 oxidation state of K for K_2CO_3 [38]. Further, the C 1 s spectra exhibited two peaks at 284.80 eV and 289.14 eV for uncalcined, 285.06 eV and 289.20 eV for calcined, along with 284.65 eV and 289.26 eV for 3rd recycled catalysts, respectively, which were attributed to the sp^2 hybridized carbonyl group of metal carbonate [45]. Similarly, the XPS spectra of Si 2p, the catalysts showed one peak each for uncalcined, calcined, and 3rd recycled catalysts at binding energies of 102.34 eV, 101.71 eV, and 102.24 eV, respectively, that belonged to the SiO_2 component in the catalysts. Basumatary et al. [73] also illustrated the existence of Si 2p in their catalyst, which has the same binding energies. Also, similar binding energies of Si 2p for two banana peel ashes were reported by Tamuli et al. [74], which were attributed to the existence of SiO_2 in the catalysts. The results of this study suggest that the catalyst contains K, C, and O in their major concentration stating that the catalysts have basic site that enhanced its catalytic property.

3.1.6. High-Resolution Transmission Electron Microscopy Analysis. The HRTEM and SAED patterns of the uncalcined (Figure 7) and calcined (Figure 8) catalysts showed a cluster of spherical and oval-shaped layouts in addition to some nonuniform structures. Fringe structures are visible in the uncalcined catalyst, which is characteristic of mesoporous nature, and this feature is in accordance with the BET analysis. DigitalMicrograph (Gatan Microscopy Suite) software was utilized to deduce the *d* values (interplanar distance) observed in the uncalcined catalyst (Figure 7(c)) which portrayed different *d* values indicating the catalyst to be polycrystalline in nature [75]. Further, the SAED pattern of the two catalysts represented in Figures 7(d) and 8(d) exhibited the catalyst's polycrystalline nature, which coincides with the *Musa acuminata* peel catalyst mentioned by Daimary et al. [4] and the *Xanthium strumarium* seed shells studied by Chutia et al. [45].

3.1.7. Study of Soluble Alkalinity, pH Value, and Basicity of the Catalyst. The soluble alkalinity of the calcined catalyst was determined from the reported procedure and was evaluated to be 2.77 mmol/g. This value of the soluble alkalinity of the catalyst can be attributed to the presence of K and Ca as elements in the form of oxides and carbonates, as specified

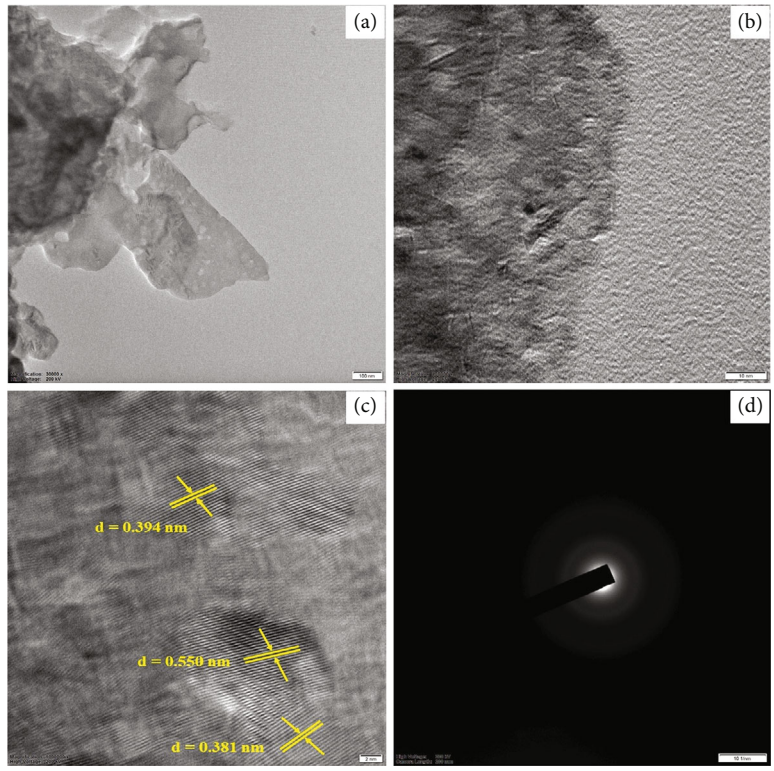

Figure 7: (a–c) HRTEM images and (d) SAED pattern of uncalcined catalyst.

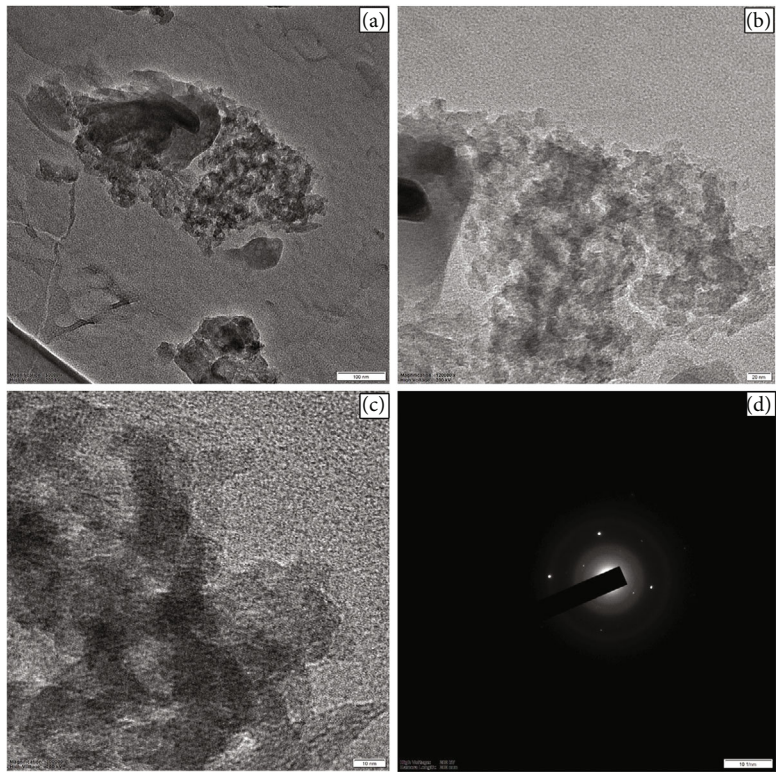

Figure 8: (a–c) HRTEM images and (d) SAED pattern of calcined catalyst.

by the XRD analysis. Mendonça et al. [75] found 3.71 mmol/g as the soluble alkalinity of waste tucumã (*Astrocaryum aculeatum* Meyer) peels catalyst calcined at 800°C. They mentioned that the specified alkalinity value was attributed to the occurrence of alkali and alkaline earth metals in abundance in their catalyst. Similarly, Barros et al. [76] found the

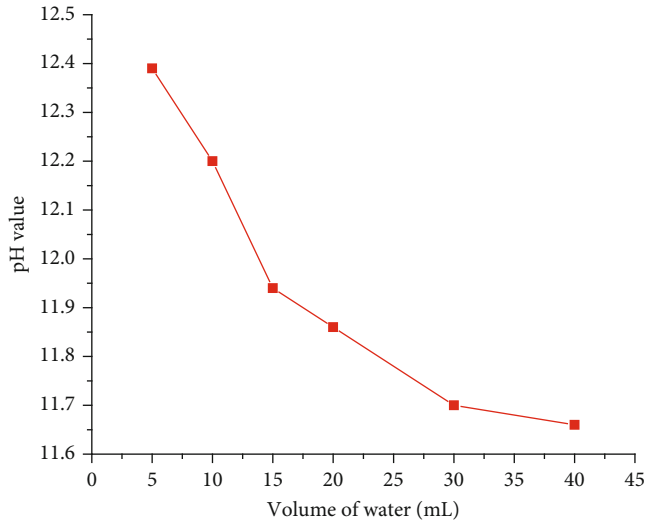

Figure 9: pH variation of calcined catalyst (1 g) at different volumes of water (mL).

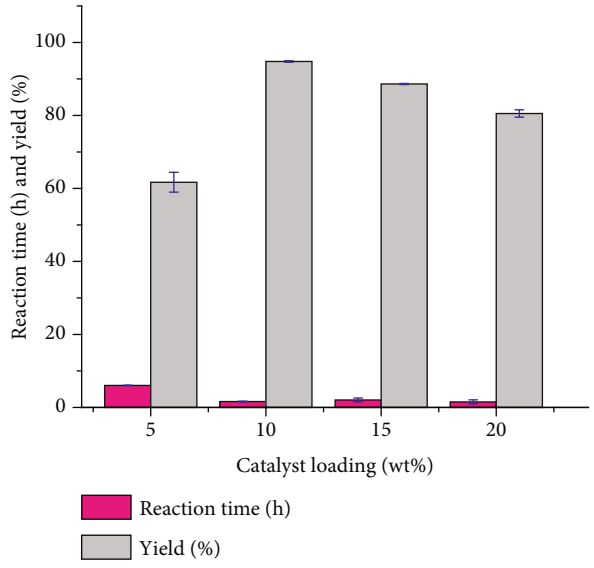

Figure 10: Effect of calcined catalyst loading on biodiesel synthesis (temperature = 65°C, MTOR = 9 : 1).

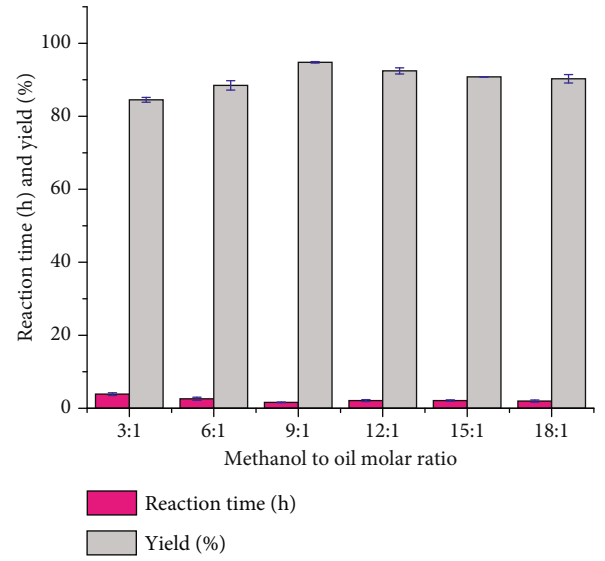

Figure 11: Effect of MTOR on biodiesel synthesis (temperature = 65°C, calcined catalyst = 10 wt%).

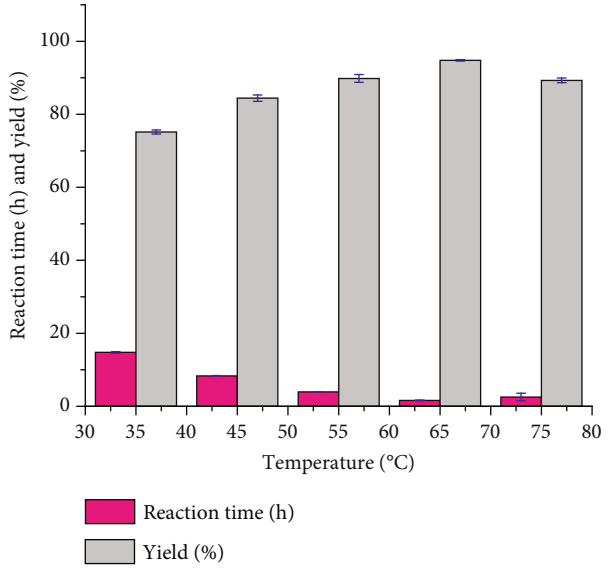

Figure 12: Effect of temperature on biodiesel synthesis (calcined catalyst = 10 wt%, MTOR = 9 : 1).

soluble alkalinity of pineapple (*Ananás comosus)* leaf catalyst as 0.39 mmol/g. Thus, the soluble alkalinity of the present catalyst is high due to the presence of K and Ca, and this outcome is in line with the XRD (Figure 2) and FTIR (Figure 4) data, which revealed the occurrence of metal carbonates and metal oxides.

The pH was determined by dissolving the calcined catalyst of 1 g in varying amounts of deionized water, as shown in Figure 9. At 1 : 5 (w/v), a pH value of 12.39 was obtained, which gradually reduced to 11.66 at 1 : 40 (w/v) stating that the catalyst's basic character declined with dilution. Similar biowaste-based catalysts are reported to have lower pH values than those of the present catalyst, for instance, *Xanthium strumarium* seed shells (pH = 12.29) [45], sugarcane bagasse (pH = 12.10) [43] and karanja seed shells (pH = 11.46) [77]. From this investigation, it can be mentioned that the catalyst has exceptional basicity.

The basicity of the calcined catalyst was determined by the Hammett technique, where the results are established based on color variation [73]. The basic strength of the catalyst in this study was observed within $10.1 < H_- < 18.4$, and a basicity of 0.13 mmol/g was determined. Catalysts with lower basicity were investigated, such as sugarcane bagasse (0.0891 mmol/g) [43], which was applicable for biodiesel production. The efficiency of the catalyst can be represented by turnover frequency (TOF) [38]. In this view, estimated basicity was utilized to calculate the turnover frequency (TOF), which was evaluated using the equation mentioned by Nath et al. [38]. The TOF of the current catalyst is

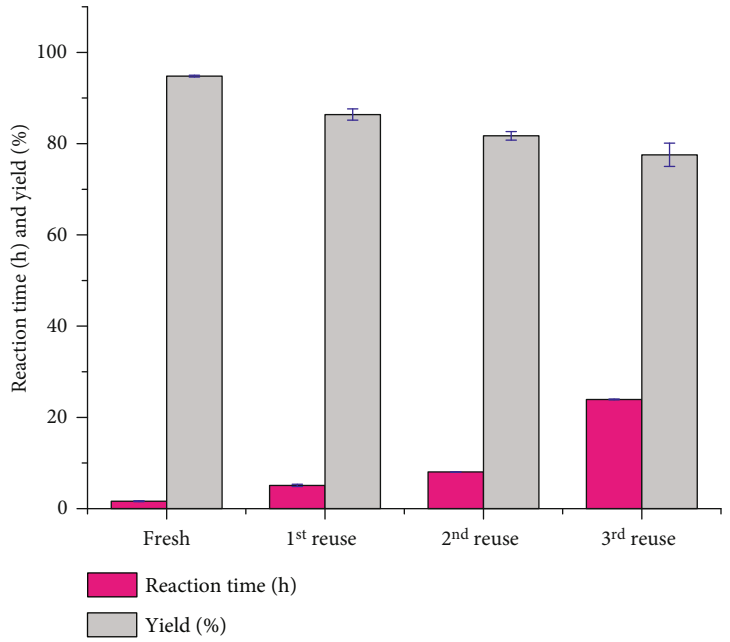

Figure 13: Reusability test of calcined catalyst (catalyst load = 10 wt%, MTOR = 9 : 1, temperature = 65°C).

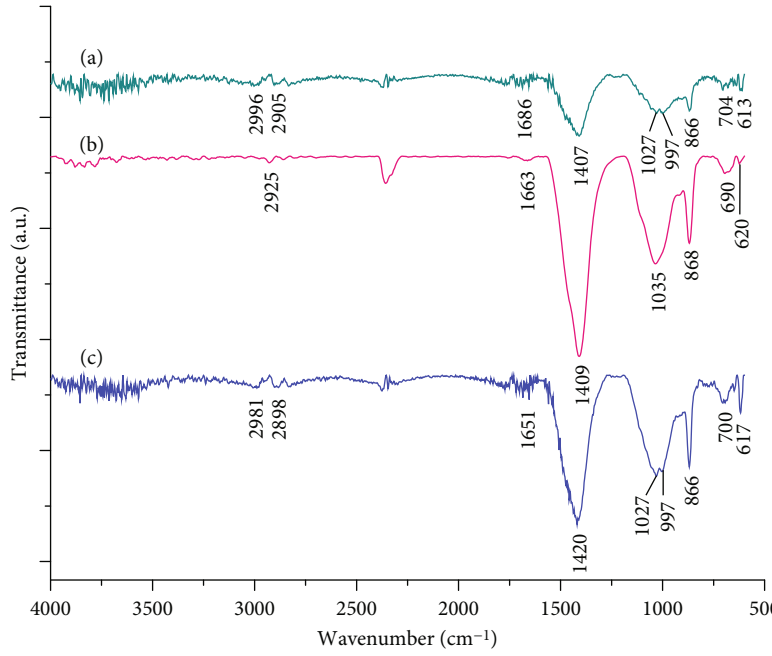

Figure 14: FT-IR spectra of (a) 1st, (b) 2nd, and (c) 3rd recycled catalysts.

estimated to be 14.57 per hour, which is significantly higher than that of *Xanthium strumarium* seed shells [45].

3.2. Catalytic Activity of Vigna mungo Catalyst. The rate and yield of biodiesel are affected by the amount of catalyst load [78]. The influence of catalyst loading in this study is represented in Figure 10, where MTOR was set to 9 : 1, temperature to 65°C, and the catalyst load was varied from 5 to 20 wt%. It was observed that on raising the catalyst loading from 5 to 10 wt%, the yield of biodiesel increased from $61.69 \pm 3.85\%$ to $94.79 \pm 0.27\%$ with a reduction in reaction time. These findings could be due to the presence of optimum numbers of the catalyst's active sites on its surface. However, on increasing the catalyst loading from 15 to 20 wt%, the biodiesel yield reduced with no considerable change in reaction time. This may be due to resistance in mass transfer in the reaction system. From an economic point of view, it is favorable to consider 10 wt% as the optimum catalyst loading. Thus, in the present study, 10 wt% was regarded as the

Table 5: Catalytic activity of *Vigna mungo* catalyst and comparison with reported ash-based catalysts in biodiesel synthesis.

Feedstock	Catalyst	Calcination time (h); temperature (°C)	Surface area ($m^2 g^{-1}$)	Parameters				Biodiesel (%)	References
				Catalyst load (wt. %)	MTOR	Temp (°C)	Time (h)		
Soybean oil–sunflower oil–canolaoil –jatropha oil–pongamia oil	Calcined *Vigna mungo* (L.) Hepper	2 h; 550°C	7.204	10	9 : 1	65	1.6 ± 0.14	94.79 ± 0.27% (Y)	This study
Clarias gariepinus–Nicotiana tabacum–Elaeis guineensis	CaO derived from agricultural waste	3 h; 900°C	1.1	5	4.15 : 1	79.68	1.33	99.19 (Y)	Adepoju et al. [26]
Rubber oil–neem oil	Elephant ear pod husk	4 h; 700°C	1.2960	2.96	11.44 : 1	150 W	0.098	98.77 (Y)	Falowo et al. [28]
Cucurbita pepo oil–*Chrysophyllum albidum* oil–papaya seed oil	*Citrullus lanatus* and *Musa acuminate* peels	4 h; 700°C	1.00	5	6.97	80	1.67	98.00 (Y)	Adepoju et al. [29]
Yellow oleander oil–rubber seed oil	Cocoa, kola nut, and fluted pumpkin husks	4 h; 500 °C	17.266	1.5	9 : 1	55	0.67	95.02 (Y)	Falowo and Betiku [39]
Waste cooking oil–refined palm oil	Fly ash	—	9.028	13.57	6.7	55	2	73.8 (Y)	Vargas et al. [92]
Jatropha curcas L. oil	*L. perpusilla* Torrey ash	2 h; (550 ± 5) °C	9.622	5	9 : 1	65 ± 5	5	89.43 (C)	Chouhan and Sarma [30]
Linseed–marula seed oil	Eggshells/banana peels	2 h; 800°C	—	3.5	15 : 1	65	1	95.03 (Y)	Etim et al. [81]
Canola oil	$LiNO_3$/Chicken bone	4 h; 850 °C	4.00 ± 0.13	4	18 : 1	60	3	96.6 (Y)	AlSharifi and Znad [22]
Waste vegetable oil	KNO_3/Oil shale ash	4 h; 700°C	1.759	10	45 : 1	65	2	100 (C)	Al-Hamamre et al. [24]
Waste frying oil	KNO_3-loaded coffee husk ash	3 h; 600°C	0.773	3	12 : 1	45	1	72.04 (Y)	Bekele et al. [84]
Waste cooking oil	KBr impregnated CaO	4 h; 900°C	—	3	12 : 1	65	1.8	83.6 (Y)	Mahesh et al. [85]
Palm oil	Waste banana peels	2 h; 600°C	—	7	15 : 1	RT	0.5	97.7 (C)	Tarigan et al. [31]
Soybean oil	Moringa leaves	2 h; 500°C	—	6	6 : 1	65	2	86.7 (Y)	Aleman-Ramirez et al. [32]
Soybean oil	Acai seed	4 h; 800°C	—	12	18 : 1	100	1	98.5 (Y)	Mares et al. [82]
Soybean oil	Cupuaçu (*Theobroma grandiflorum*) seeds	4 h; 800°C	—	10	10 : 1	80	8	98.36 (C)	Mendonça et al. [83]
Used cooking oil	ZnO supported coal fly ash	4.5 h; 400 °C	58.76	0.5	12 : 1	140	3	83.17 (Y)	Yusuff et al. [86]
Soybean oil	ZrO_2-supported bamboo leaf ash (ZrO_2/BLA)	4 h; 400 °C	56.12	12	15 : 1	Reflux	15	96.75 (Y)	Fatimah et al. [102]
Soybean oil	ZrO_2-supported bamboo leaf ash (ZrO_2/BLA)	4 h; 400 °C	56.12	12	15 : 1	MW	0.5	95.99 (Y)	Fatimah et al. [102]

h: hour; temp: temperature; Y: yield; C: conversion.

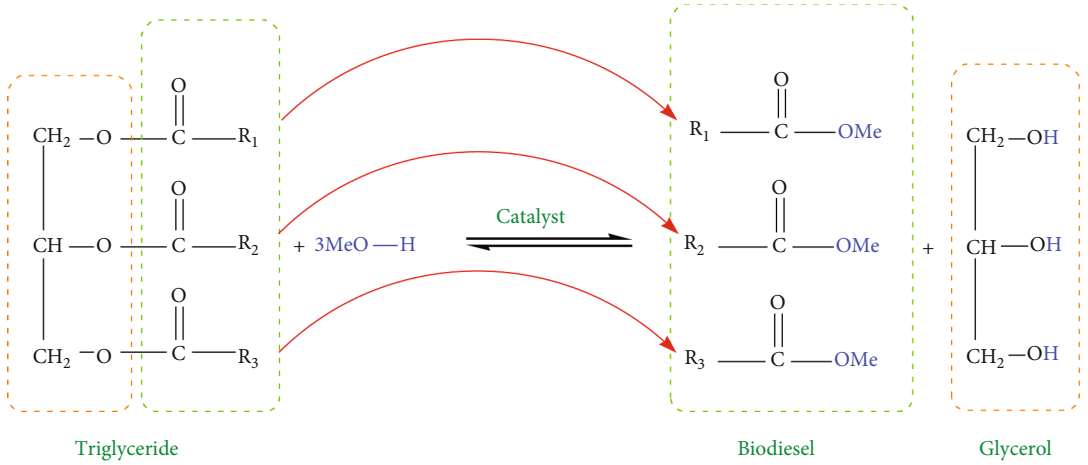

Figure 15: Reactions involved in catalytic transesterification.

best catalyst loading as it produced 94.79 ± 0.27% of maximum biodiesel yield in 1.6 ± 0.14 h.

The effect of MTOR was carried out by fixing 10 wt% of catalyst loading at 65°C, which is shown in Figure 11. In this investigation, it was found that on increasing the MTOR from 3 : 1 to 9 : 1, the product yield enhanced from 84.52 ± 0.93% to 94.79 ± 0.27%. Since transesterification is a reversible reaction, high MTOR is crucial to shift the equilibrium reaction in a forward direction [38]. On further increasing the MTOR from 12 : 1 to 15 : 1, a reduction in the biodiesel yield was observed. This can be owed to less interaction of the catalyst with the reactants due to dilution. Therefore, MTOR of 9 : 1 was regarded as the optimum MTOR in this study.

The influence of different reaction temperatures is represented in Figure 12. On elevating the temperature from 35°C to 65°C, the biodiesel yield increased from 75.17 ± 0.79% to 94.79 ± 0.27%. High temperature is favored as the transesterification reaction is endothermic in nature, which accelerates the miscibility and mass transfer in the reaction system [79]. Also, high temperature shifts the equilibrium in a forward direction [80]. In the present study, at temperature beyond 65°C, the biodiesel yield was reduced. This outcome can be credited to the vaporization of methanol, which led to a decline in the methoxide ions in the reaction mixture [43]. Thus, 65°C was regarded as the optimum reaction temperature in this study.

The catalyst's reusability was studied by preparing 100 mL of biodiesel at the optimum reaction conditions (10 wt% of catalyst loading, 9 : 1 MTOR, and 65°C of reaction temperature). Following completion of the reaction, the catalyst was extracted from the reaction mixture via filtration with the aid of a suction pump, followed by washing several times with petroleum ether and then with acetone. Subsequently, the catalyst was dried for 4 h at 110°C in an air oven and then stored in a desiccator and employed in the following cycle. Then, the reaction was performed by using the catalyst under optimum conditions to study its reusability. This method is used for each cycle. The outcomes are represented in Figure 13, where it is noticeable that the catalyst retained its catalytic activity for two cycles. However, on the third run, the yield of biodiesel was slightly reduced with a considerable increase in reaction time. This result could be due to the deposition of unreacted oil or glycerol on the catalyst's surface. From the FESEM images of the 3rd recycled catalyst (Figures 5(g) and 5(h)), the morphology of the catalyst completely changed in contrast to the calcined catalyst. Sheet-like layered structures of varying shapes are visible in the images, which demonstrate the coating of glycerol on the catalyst's surface. Another reason could be the leaching of active elements from the catalyst's surface, such as K and Ca, which are evident from the FESEM-EDX (Figures 5(c), 5(f), and 5(i)), where a reduction in the weight % (Table 3) of K and Ca was observed. The weight % of K was reduced from 17.42% (calcined catalyst) to 0.94% (3rd recycled catalyst), as was the weight % of Ca reduced from 17.96% (calcined catalyst) to 0.71% (3rd recycled catalyst). A similar pattern was observed in the XPS (Figure 6) analysis, where the atomic % of K, which was 9.96% for the calcined catalyst, was reduced to 3.98% for the 3rd recycled catalyst. Similarly, from the XRD (Figure 2) data for calcined and 3rd recycled catalysts, the disappearance of peak and decrease in peak intensities resembling the leaching of active components are evident. Further, FT-IR analysis done for the catalysts recycled in three stages (for three respective recycles, *viz.*, 1st, 2nd, and 3rd recycle) is depicted in Figure 14. From the FT-IR spectra, changes in peak along with reduced peak intensities are noticed for the peak in the region 1690-1400 per cm indicating C=O stretching of the carbonyl group, which is probably due to metal carbonate leaching. Also, peaks in the range of 2900-3000 per cm are observed, which are due to the hydrocarbon chain of glycerol deposition on the catalyst's surface, which is responsible for blocking the catalyst's active site and thereby declining the catalytic efficacy. It can be concluded that the leaching of active elements and blockage of the catalyst's active sites by oil or glycerol have limited the reusability of the catalyst up to three cycles.

3.2.1. Comparison of the Present Study with Published Results. The catalytic ability of our current catalyst is evaluated in relation to other heterogeneous (ash based) catalysts, which are mentioned in Table 5, in terms of catalytic

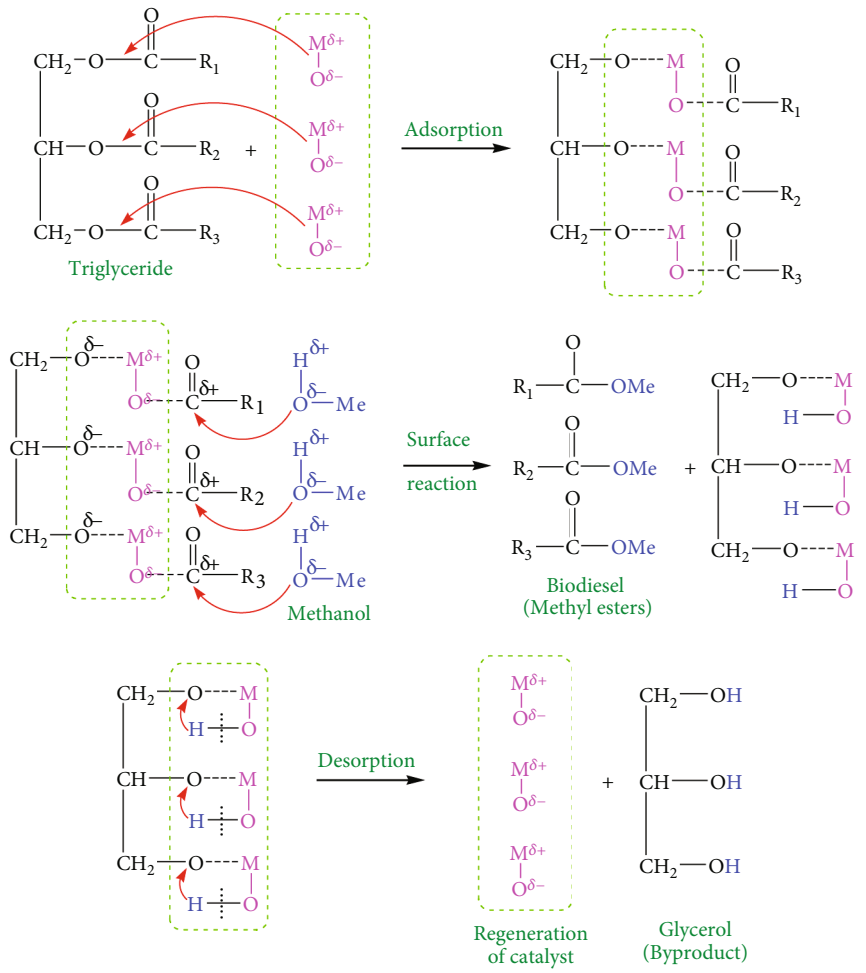

Figure 16: Plausible reaction mechanism using *Vigna mungo* derived catalyst in transesterification of oil with methanol to biodiesel [17].

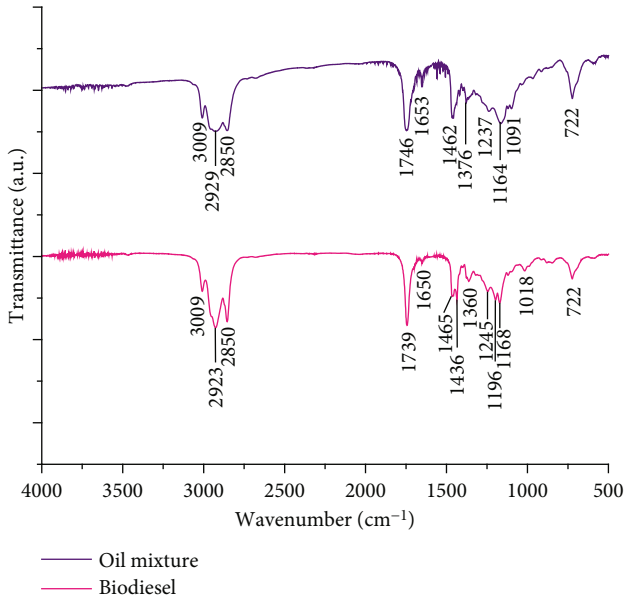

Figure 17: FT-IR spectra of oil mixture and its biodiesel.

Table 6: FT-IR analysis of biodiesel.

Wave number (cm^{-1})	Functional group
3009	=C–H stretching of alkene
2929-2850	Symmetric and asymmetric C–H stretching of alkane
1739	C=O stretching of methyl ester
1650	C=C stretching vibration of alkene
1465-1360	CH_3 deformation
1300-1000	C–O stretching vibration
722	$-CH_2-$ rocking vibration

efficiency. The optimal reaction parameters of a variety of biomass-based catalysts are displayed in Table 5, which have demonstrated high efficiency in producing more than 90% of biodiesel from single and mixed feedstocks. For catalyst preparation, high calcination temperatures and long calcination times are not economically feasible for industrial-scale production [72]. The calcination conditions of this study (550°C, 2 h) are lower than the calcination conditions cited by Adepoju et al. [29], Adepoju et al. [26], Etim et al. [81], Mares et al. [82], and Mendonça et al. [83], which were ≥600°C, 2-4 h. A good biodiesel production has also been

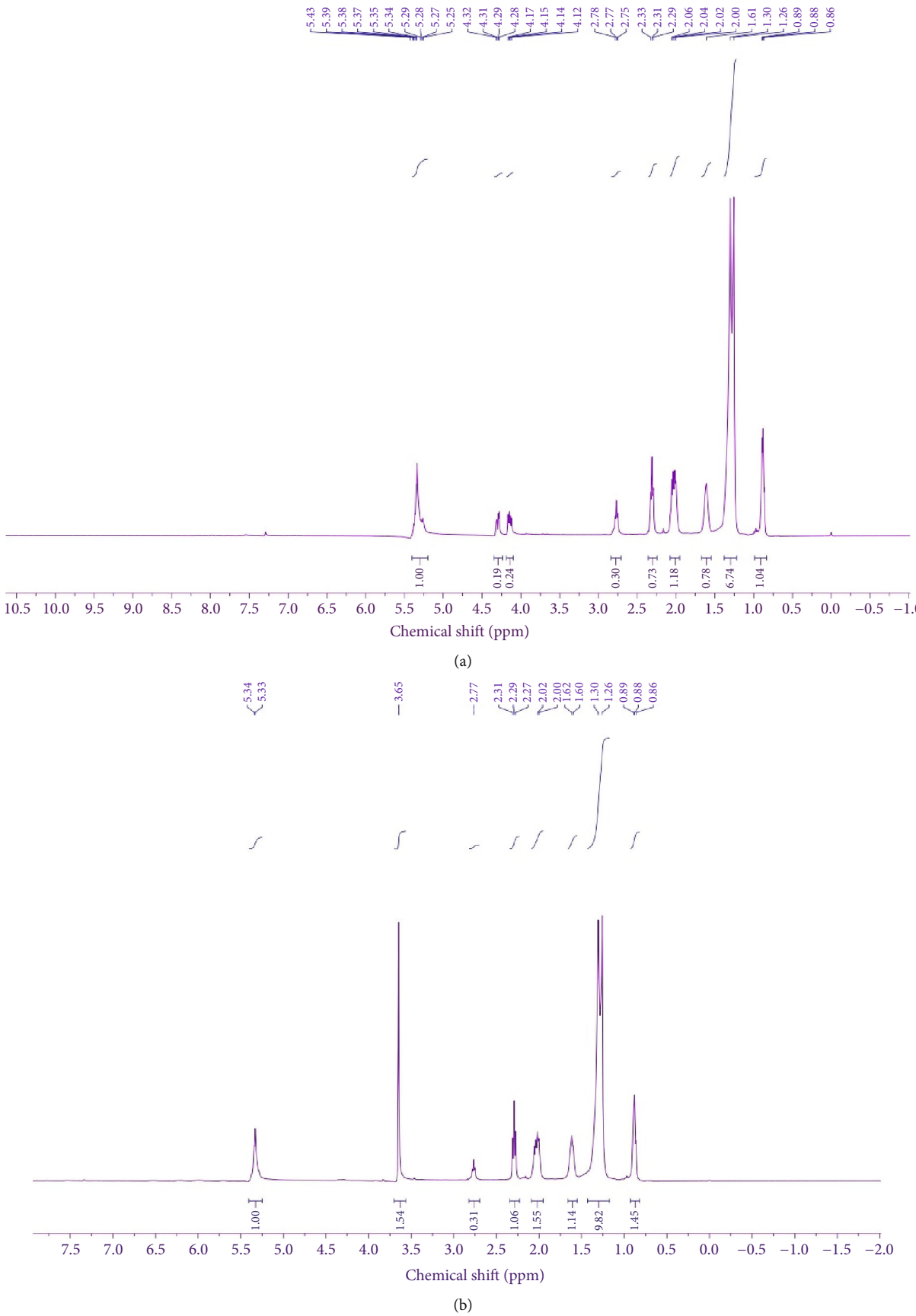

Figure 18: ^{1}H NMR of (a) oil mixture and (b) biodiesel.

Table 7: ^{1}H NMR spectrum analyses of oil mixture and biodiesel.

Types of protons/carbons	Triglyceride (oil) ^{1}H (δ, ppm)	Biodiesel ^{1}H (δ, ppm)
Olefinic protons (–CH=CH–)	5.34-5.43	5.33-5.34
Methine proton at C2 of glycerides (–CH–CO_2R)	5.25-5.29	—
Methylene protons at C1 and C3 of glycerides (–CH_2–CO_2R)	4.12-4.32	—
Methoxy protons (-$COOCH_3$) of ester	—	3.65
Bis-allylic protons (–C=C–CH_2–C=C–)	2.75-2.78	2.77
α-methylene to ester (–CH_2–CO_2R)	2.31	2.27-2.31
α-methylene to double bond (–CH_2–C=C–)	2.02-2.06	2.00-2.02
β-methylene to ester (CH_2–C–CO_2R)	1.61	1.60-1.62
Backbone methylene's –$(CH_2)_n$–	1.26-1.30	1.26-1.30
Terminal methyl protons (C–CH_3)	0.86-0.89	0.86-0.89

observed for catalysts such as *L. perpusilla* Torrey ash [30], waste banana peels [31], moringa leaves [32], mixture of *Citrullus lanatus* with *Musa acuminate* peels [29], and blend of cocoa-kola nut-fluted pumpkin husks [39], which are summarized in Table 5. The authors stated alkali and alkaline earth metals as the major ingredients in their catalysts for showcasing such high catalytic ability. Similarly, in our present catalyst, K and Ca were the main components of the catalyst's efficiency, and this is evident from EDX analysis (Table 3). From Table 5, it can be seen that the BET surface area reported in the studies of Chouhan and Sarma [30], Bekele et al. [84], Mahesh et al. [85], Aleman-Ramirez et al. [32], and Yusuff et al. [86] is lower in contrast to the current study (7.204 m^2/g). This could be the cause of the current study's improved catalytic activity. Additionally, the other heterogeneous catalysts, such as CaO derived from agricultural waste [26], $LiNO_3$/chicken bone [21], KNO_3/oil shale ash [22], KNO_3-loaded coffee-husk ash [84], and KBr-impregnated CaO [85], are highly selective towards the transesterification reaction. However, their principal disadvantages are that they require high expenses and drastic reaction conditions for their preparation. Due to the catalyst's availability as natural waste and did not involve use the of any hazardous chemicals or rigorous reaction conditions, the catalyst preparation in this work was inexpensive. Among the various heterogeneous catalysts indicated in the table, the calcined *Vigna mungo* catalyst also demonstrated good catalytic activity in terms of reaction temperature, biodiesel yield, and reaction time. This might be due to the high amount of K and Ca content in it, along with its high basicity (0.13 mmol/g) and TOF of 14.57 per h. In this study, the solid catalyst developed for utilization in the transesterification reaction (Figure 15) is composed of metal oxides and metal carbonates. It can be expected that the transesterification of homogeneous oil mixture with methanol using the developed base catalyst follows the Eley-Rideal reaction steps as depicted in Figure 16 [17, 43].

3.3. Limitations and Practical Implication of the Study. Heterogeneous catalysts provide active sites with the reactants under reaction temperature. These catalysts neither get consumed nor dissolved during the course of the reaction, making them reusable for the next cycle. The calcined *Vigna mungo* (L.) Hepper catalyst actively transesterified the homogeneous oil mixture. The efficiency of its activity could be credited to the presence of K and Ca, which yielded $94.79 \pm 0.27\%$ of biodiesel in 1.6 ± 0.14 h. But during the reusability test, it was determined that the catalyst may be used for up to three consecutive cycles. This is because the catalyst's catalytic efficiency is reduced due to the active components eroding from its surface.

The most commercially viable kinds of heterogeneous catalysts are those derived from agricultural waste. The catalyst developed in this study is an environmentally friendly material because it is derived from natural resources and will not harm the environment when it is widely deposited after use [38]. The costs associated with creating catalysts can be decreased since the leftover parts of *Vigna mungo* are widely available as agricultural waste. Its strong catalytic activity further suggests using it as a heterogeneous catalyst for the large-scale production of biodiesel. However, the magnetization of the catalyst would have increased its reusability by making it simpler to separate and regenerate for additional usage. It is possible to increase the catalyst's reusability by modifying the catalyst at a low cost to stop it from leaching [38]. Additionally, the catalyst's water extract can be utilized as a green solvent for organic synthesis or as a precursor for the metal oxide nanoparticle synthesis [87]. The catalyst can also be used as an adsorbent for the removal of heavy metals and dyes or for the treatment of wastewater. Furthermore, it can serve as a basis for the preparation of numerous materials, including zeolite, graphene oxide, and activated carbon.

3.4. Characterization of Biodiesel

3.4.1. Fourier Transform Infrared Spectroscopy, Proton Nuclear Magnetic Resonance, and Gas Chromatography-Mass Spectrometry Analyses. Figure 17 depicts the FT-IR spectra of the oil mixture and biodiesel. The stretching vibration of the C=O group in the oil mixture is seen from the absorption peak at 1746 per cm, which shifted to 1739 per cm in the biodiesel due to C=O stretching of methyl ester, indicating oil mixture to biodiesel conversion (Table 6).

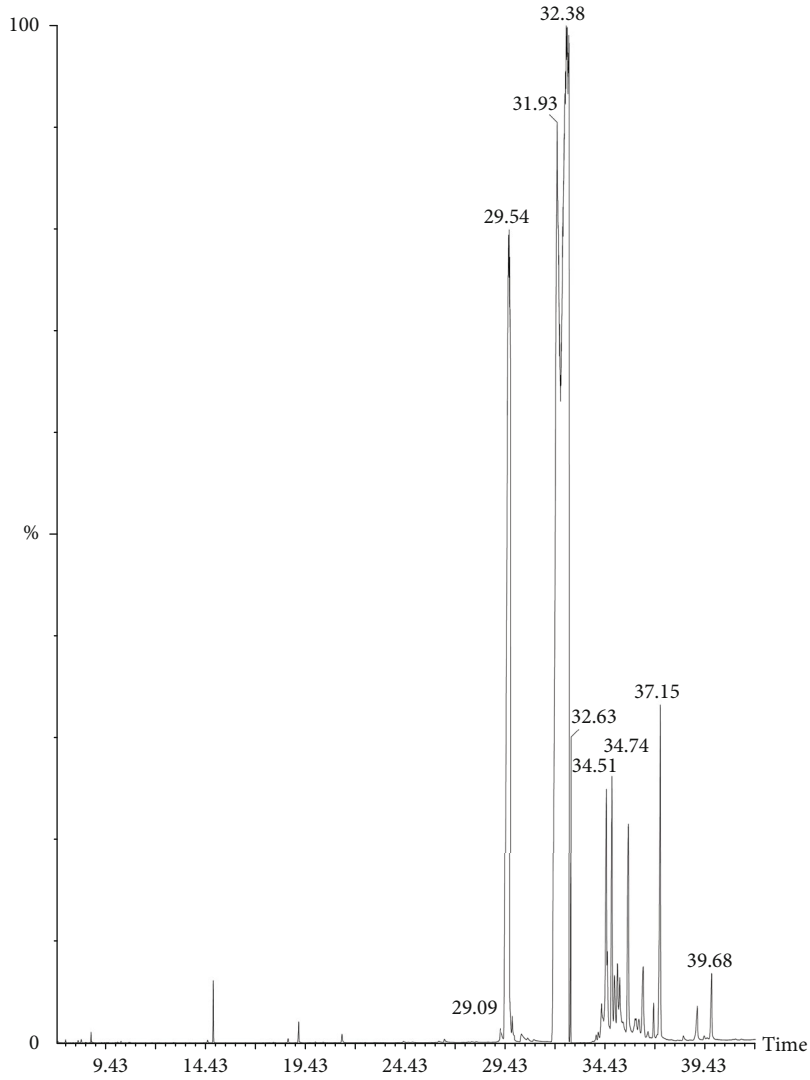

Figure 19: Gas chromatogram of produced biodiesel.

The band at 3009 per cm seen in the oil mixture and biodiesel indicates the =C–H stretching of alkene (–CH=CH–) in their fatty acid chains. The symmetric and asymmetric C–H stretching of alkane in the oil mixture and biodiesel are described by the bands of region 2929-2850 per cm. The peaks at 1651 and 1650 per cm of triglyceride and product are due to the C=C stretching vibration of the alkene group. The antisymmetric and symmetric deformation vibrations of CH_3 are seen at 1462 and 1376 per cm for the oil mixture and at 1465, 1436, and 1360 per cm for biodiesel (Table 6). The transformation of the CH_2O group of triglycerides to the CH_3O group of products, as well as the stretching vibration of C–O in the oil mixture and that of biodiesel, is seen in the region from 1300-1000 per cm [14]. The IR peak at 722 per cm in the oil mixture and biodiesel is due to the rocking vibration of the $–CH_2–$ group of the fatty acid chain.

After the transesterification reaction was complete, the resultant biodiesel was confirmed by ^1H NMR analysis, which is shown in Figure 18, and the different signals are listed in Table 7. The appearance of peaks at 5.34-5.43 ppm and 5.33-5.34 ppm confirmed the presence of olefinic protons in the oil mixture and biodiesel, respectively. The peaks at 5.25-5.29 ppm and 4.12-4.32 ppm due to glyceride protons in the oil mixture are seen to disappear, while a new peak

Table 8: Composition of the biodiesel obtained from the oil mixture.

Retention time (min)	FAME	Composition (%)
29.09	Methyl palmitoleate (C16:1)	0.184
29.54	Methyl palmitate (C16:0)	17.931
31.93	Methyl linoleate (C18:2)	26.255
32.38	Methyl oleate (C18:1)	44.839
32.63	Methyl stearate (C18:0)	0.634
34.51	Methyl gondoate (C20:1)	0.439
34.74	Methyl arachidate (C20:0)	1.492
37.15	Methyl behenate (C22:0)	2.329
39.68	Methyl lignocerate (C24:0)	0.497

Table 9: Comparison of physicochemical properties of produced biodiesel with standards and reported mixed oil biodiesels.

Properties	Biodiesel from oil mixture (this study)	ASTM D6751	EN 14214	Reported biodiesels from various mixed oil feedstocks						
				Kusumo et al. [12]	Falowo et al. [28]	Karmakar et al. [41]	Fadhil et al. [91]	Vinayaka et al. [90]	Adepoju et al. [88]	Ong et al. [89]
Density (g/cm^3)	0.8792	NS	0.86–0.90	0.878	0.897	0.816	0.8989	0.82	0.872	0.866
Kinematic viscosity (40 °C, mm^2/s)	4.231	1.9–6.0	3.5–5.0	4.89	5.94	2.4	3.61	4.5	1.82	3.72
Cetane index	57.416	NS	NS	—	—	—	—	—	—	—
Saponification number (mg KOH/g of oil)	181.34	—	—	—	—	—	175.24	—	178.24	—
API	29.12	36.95	NS	—	22.81	—	—	—	—	—
Aniline point (°F)	226.15	331	NS	—	283.34	122	—	—	—	—
Diesel index	65.86	50.4	NS		64.63	57.78	—	—	75.53	—
HHV (MJ/kg)	40.73	35 (min)	35 (min)	40.17	—	—	40.88	—	41.27	41.43
IV (mg/100 g)	84.37		120 (max)	—	68.33	—	91.0	—	52.62	—

NS: not specified; API: American petroleum index; HHV: higher heating value; IV: iodine value; min: minimum; max: maximum.

appeared at 3.65 ppm in the biodiesel clearly confirmed the conversion of the oil mixture to product. The singlet peak at 3.65 ppm is because of the methoxy protons of the biodiesel. Also from Figure 18, a triplet peak at 2.31 ppm is seen, which belongs to α–CH_2 protons. The oil conversion (%) is calculated for the transesterification reaction carried out under optimum reaction conditions using equation (2) and is found to be 96.86%.

The fatty acid profile of biodiesel synthesized from the oil mixture is represented in Figure 19. A total of nine unsaturated and saturated fatty acids are detected by the GCMS technique (Table 8). The most dominant methyl ester was methyl oleate (43.77%), which is an unsaturated fatty acid ester, followed by methyl linoleate (25.65%) and methyl palmitate (17.50%). The other fatty acids are methyl palmitoleate (0.18%), methyl stearate (0.62%), methyl gondoate (0.43%), methyl arachidate (1.46%), methyl behenate (2.27%), and methyl lignocerate (0.49%).

3.4.2. Biodiesel Properties. The physicochemical characteristics of the biodiesel obtained in this study are listed in Table 9 along with the biodiesel specifications, *viz.*, ASTM D6751 and EN 14214. For comparison, Table 9 also shows the physicochemical characteristics of reported biodiesels made from different combinations of feedstock. The density of the biodiesel obtained in this study is found to be 0.8792 g/cm^3 which is in the limits of biodiesel standards, and it is also comparable to the density of the biodiesel reported by Kusumo et al. [12], Karmakar et al. [41], Adepoju et al. [88], and Ong et al. [89]. This study's kinematic viscosity is determined to be 4.231 mm^2/s, satisfying the ASTM and EN standards. However, higher kinematic viscosity was revealed in the biodiesel prepared from the combination of neem with rubber seed oil [28] and the mixture of pongamia-neem oil [90]. In the current study, the cetane index is calculated using the equation mentioned in Table 2 and is found to be 57.416. Further, the saponification number in the current study is obtained as 181.34 mg/KOH, which is almost parallel to that of the biodiesel-synthesized mixture of castor seed-waste fish oil [91] and a mixture of *Citrus sinensis-Hibiscus sabdariffa-Carica papaya*-waste used oils [88]. The measure of the degree of unsaturation is indicated by the iodine value (IV), and an IV of 84.37 is observed in this current study. The higher heating value (HHV) was also derived for the biodiesel obtained in this study, which was found to be 40.73 MJ/kg. Further, other physicochemical properties like diesel index, API, and aniline point were also determined, which were recorded as 65.86, 29.12, and 226.15, respectively. Lastly, as seen in Table 9, the biodiesel obtained in this current study, which is derived from the blend of five different edible and inedible oils, satisfies the aforesaid biodiesel standards.

4. Conclusions and Recommendations

This study used a combination of different edible and inedible oils as the feedstock to produce biodiesel utilizing a low-cost, renewable, and recyclable solid catalyst made from the leftovers of black grams (*Vigna mungo* (L.) Hepper). The characterization studies (such as XRD, FT-IR, XPS, and FESEM-EDX) revealed the presence of K and Ca as carbonates and oxides in the catalysts. Also, the mesoporous nature of the calcined catalyst was also obvious from the BET and HRTEM analyses. The basic strength determined via the Hammett method showed basicity within $10.1 < H_- < 18.4$ with 0.13 mmol/g and a TOF of 14.57 per hour. The maximum biodiesel yield and oil conversion of 94.79 ± 0.27% and 96.86%, respectively, were attained under the optimum reaction parameters of 10 wt% of catalyst concentration, 9 : 1 of MTOR, 65°C of reaction temperature, and 1.6 ± 0.14 h of reaction time. Due to the leaching of active components, the catalyst was reusable for up to three consecutive rounds yielding 77.54 ± 3.62% of biodiesel, which supports its ability to be used for large-scale production. Further, the GC MS study revealed the occurrence of different saturated as well as unsaturated fatty acids in the methyl ester. Thus, from all these observations, it is evident that the agricultural waste developed in this study is an environmentally benign as well as cost-efficient heterogenous catalyst for large-scale biodiesel synthesis from mixture of different oils. It can be recommended for applications in waste-water treatment and chemical transformations. It is also possible to suggest that the catalyst be modified via various techniques or blended with other ash-based catalysts in order to increase the catalyst's efficiency. It may eventually take the place of homogeneous catalysts due to its simplicity and reduced posttreatment processes.

Abbreviations

^{1}H HMR: Proton nuclear magnetic resonance
API: American petroleum index
ASTM: American Society for Testing and Materials
BET: Brunauer-Emmett-Teller
BJH: Barrett-Joyner-Halenda
EDX: Energy dispersive X-ray spectroscopy
EN: European standards
FAME: Fatty acid methyl ester
FESEM: Field emission scanning electron microscopy
FFA: Free fatty acid
FT-IR: Fourier transform infrared spectroscopy
GC-MS: Gas chromatography-mass spectrometry
HHV: Higher heating value
HRTEM: High-resolution transmission electron microscopy
IR: Infrared
IV: Iodine value
MTOR: Methanol to oil molar ratio
SAED: Selected area electron diffraction
TLC: Thin layer chromatography
TOF: Turnover frequency
WCO: Waste cooking oil
XPS: X-ray photoelectron spectroscopy
XRD: X-ray diffraction.

Data Availability

The data used to support the findings of this study are available from the corresponding author upon request.

Conflicts of Interest

The authors declare that there are no conflicts of interest regarding the publication of this article.

Acknowledgments

The authors extend their appreciation to the Deanship of Research and Graduate Studies at King Khalid University for funding this work through the Large Research Group under grant number R.G.P. 2/329/45. The authors acknowledge MARC, Bangalore; SAIF, NEHU, Shillong; CSIR-NEIST, Jorhat; Biotech Park, Guwahati; Department of Chemistry (Gauhati University); CIF; NIT Silchar; and CIT, Kokrajhar, India, for the analyses of catalysts and biodiesel. S. Brahma thanks the Ministry of Tribal Affairs, Govt. of India, for the NFST fellowship during the PhD research work.

References

[1] O. Awogbemi, F. Inambao, and E. I. Onuh, "Modification and characterization of chicken eggshell for possible catalytic applications," *Heliyon*, vol. 6, no. 10, article e05283, 2020.

[2] C. W. Su, X. Yuan, R. Tao, and X. Shao, "Time and frequency domain connectedness analysis of the energy transformation under climate policy," *Technological Forecasting and Social Change*, vol. 184, article 121978, 2022.

[3] O. Awogbemi, D. V. V. Kallon, and V. S. Aigbodion, "Trends in the development and utilization of agricultural wastes as heterogeneous catalyst for biodiesel production," *Journal of the Energy Institute*, vol. 98, pp. 244–258, 2021.

[4] N. Daimary, P. Boruah, K. S. H. Eldiehy et al., "*Musa acuminata* peel: a bioresource for bio-oil and by-product utilization as a sustainable source of renewable green catalyst for biodiesel production," *Renewable Energy*, vol. 187, pp. 450–462, 2022.

[5] I. Veza, Z. Zainuddin, N. Tamaldin, M. Idris, I. Irianto, and I. M. R. Fattah, "Effect of palm oil biodiesel blends (B10 and B20) on physical and mechanical properties of nitrile rubber elastomer," *Results in Engineering*, vol. 16, article 100787, 2022.

[6] Y. C. Sharma and B. Singh, "A hybrid feedstock for a very efficient preparation of biodiesel," *Fuel Processing Technology*, vol. 91, no. 10, pp. 1267–1273, 2010.

[7] J. G. E. Guedes Júnior, F. R. Mattos, G. J. Sabi et al., "Design of a sustainable process for enzymatic production of ethylene glycol diesters via hydroesterification of used soybean cooking oil," *Journal of Environmental Chemical Engineering*, vol. 10, no. 1, article 107062, 2022.

[8] J. Gupta, M. Agarwal, and A. K. Dalai, "Intensified transesterification of mixture of edible and nonedible oils in reverse flow helical coil reactor for biodiesel production," *Renewable Energy*, vol. 134, pp. 509–525, 2019.

[9] I. Simbi, U. O. Aigbe, O. Oyekola, and O. A. Osibote, "Optimization of biodiesel produced from waste sunflower cooking oil over bi-functional catalyst," *Results in Engineering*, vol. 13, article 100374, 2022.

[10] S. Brahma, B. Nath, B. Basumatary et al., "Biodiesel production from mixed oils: a sustainable approach towards industrial biofuel production," *Chemical Engineering Journal Advances*, vol. 10, article 100284, 2022.

[11] F. Toldrá-Reig, L. Mora, and F. Toldrá, "Trends in biodiesel production from animal fat waste," *Applied Sciences*, vol. 10, no. 10, p. 3644, 2020.

[12] F. Kusumo, T. M. Mahlia, A. H. Shamsuddin et al., "Optimisation of biodiesel production from mixedSterculia foetidaand rice bran oil," *International Journal of Ambient Energy*, vol. 43, no. 1, pp. 4380–4390, 2022.

[13] D. da Costa Barbosa, T. M. Serra, S. M. Plentz Meneghetti, and M. R. Meneghetti, "Biodiesel production by ethanolysis of mixed castor and soybean oils," *Fuel*, vol. 89, no. 12, pp. 3791–3794, 2010.

[14] A. Saydut, S. Erdogan, A. B. Kafadar, C. Kaya, F. Aydin, and C. Hamamci, "Process optimization for production of biodiesel from hazelnut oil, sunflower oil and their hybrid feedstock," *Fuel*, vol. 183, pp. 512–517, 2016.

[15] A. K. Ayoob and A. B. Fadhil, "Valorization of waste tires in the synthesis of an effective carbon-based catalyst for biodiesel production from a mixture of non-edible oils," *Fuel*, vol. 264, article 116754, 2020.

[16] S. M. Dharma, H. H. Masjuki, H. C. Ong et al., "Optimization of biodiesel production process for mixed *Jatropha curcas–Ceiba pentandra* biodiesel using response surface methodology," *Energy Conversion and Management*, vol. 115, pp. 178–190, 2016.

[17] S. Brahma, B. Basumatary, S. F. Basumatary et al., "Biodiesel production from quinary oil mixture using highly efficient *Musa chinensis* based heterogeneous catalyst," *Fuel*, vol. 336, article 127150, 2023.

[18] Y. C. Sharma and B. Singh, "Development of biodiesel: current scenario," *Renewable and Sustainable Energy Reviews*, vol. 13, no. 6-7, pp. 1646–1651, 2009.

[19] V. Liberato, C. Benevenuti, F. Coelho et al., "*Clostridium sp.* as bio-catalyst for fuels and chemicals production in a biorefinery context," *Catalysts*, vol. 9, no. 11, p. 962, 2019.

[20] J. Sebastian, C. Muraleedharan, and A. Santhiagu, "A comparative study between chemical and enzymatic transesterification of high free fatty acid contained rubber seed oil for biodiesel production," *Cogent Engineering*, vol. 3, no. 1, article 1178370, 2016.

[21] M. Sarno and M. Iuliano, "Active biocatalyst for biodiesel production from spent coffee ground," *Bioresource Technology*, vol. 266, pp. 431–438, 2018.

[22] A. Selemani and G. G. Kombe, "Glycerolysis of high free fatty acid oil by heterogeneous catalyst for biodiesel production," *Results in Engineering*, vol. 16, article 100602, 2022.

[23] M. AlSharifi and H. Znad, "Development of a lithium based chicken bone (Li-Cb) composite as an efficient catalyst for biodiesel production," *Renewable Energy*, vol. 136, pp. 856–864, 2019.

[24] Z. Al-Hamamre, A. Sandouqa, B. Al-Saida, R. A. Shawabkeh, and M. Alnaief, "Biodiesel production from waste cooking oil using heterogeneous KNO_3/oil shale ash catalyst," *Renewable Energy*, vol. 211, pp. 470–483, 2023.

[25] J. V. Ruatpuia, G. Halder, S. Mohan et al., "Microwave-assisted biodiesel production using ZIF-8 MOF-derived nanocatalyst: a process optimization, kinetics, thermodynamics and life cycle cost analysis," *Energy Conversion and Management*, vol. 292, article 117418, 2023.

[26] T. F. Adepoju, H. A. Akens, and E. B. Ekeinde, "Synthesis of biodiesel from blend of seeds oil-animal fat employing agricultural wastes as base catalyst," *Case Studies in Chemical*

and Environmental Engineering, vol. 5, article 100202, 2022.

[27] T. W. Riyadi, M. Spraggon, S. G. Herawan et al., "Biodiesel for HCCI engine: prospects and challenges of sustainability biodiesel for energy transition," *Results in Engineering*, vol. 17, article 100916, 2023.

[28] O. A. Falowo, M. I. Oloko-Oba, and E. Betiku, "Biodiesel production intensification via microwave irradiation-assisted transesterification of oil blend using nanoparticles from elephant-ear tree pod husk as a base heterogeneous catalyst," *Chemical Engineering and Processing*, vol. 140, pp. 157–170, 2019.

[29] T. F. Adepoju, M. A. Ibeh, U. Ekanem, and A. J. Asuquo, "Data on the derived mesoporous based catalyst for the synthesized of fatty acid methyl ester (FAME) from ternary oil blend: an optimization approach," *Data in Brief*, vol. 30, article 105514, 2020.

[30] A. P. Chouhan and A. K. Sarma, "Biodiesel production from *Jatropha curcas* L. oil using *Lemna perpusilla* Torrey ash as heterogeneous catalyst," *Biomass and Bioenergy*, vol. 55, pp. 386–389, 2013.

[31] J. B. Tarigan, S. Perangin-Angin, S. R. Simanungkalit, N. P. Zega, and E. K. Sitepu, "Utilization of waste banana peels as heterogeneous catalysts in room-temperature biodiesel production using a homogenizer," *RSC Advances*, vol. 13, no. 9, pp. 6217–6224, 2023.

[32] J. L. Aleman-Ramirez, J. Moreira, S. Torres-Arellano, A. Longoria, P. U. Okoye, and P. J. Sebastian, "Preparation of a heterogeneous catalyst from moringa leaves as a sustainable precursor for biodiesel production," *Fuel*, vol. 284, article 118983, 2021.

[33] M. Balajii and S. Niju, "A novel biobased heterogeneous catalyst derived from *Musa acuminata* peduncle for biodiesel production–process optimization using central composite design," *Energy Conversion and Management*, vol. 189, pp. 118–131, 2019.

[34] E. Betiku, A. A. Okeleye, N. B. Ishola, A. S. Osunleke, and T. V. Ojumu, "Development of a novel mesoporous biocatalyst derived from kola nut pod husk for conversion of kariya seed oil to methyl esters: a case of synthesis, modeling and optimization studies," *Catalysis Letters*, vol. 149, no. 7, pp. 1772–1787, 2019.

[35] B. Changmai, R. Rano, C. Vanlalveni, and S. L. Rokhum, "A novel *Citrus sinensis* peel ash coated magnetic nanoparticles as an easily recoverable solid catalyst for biodiesel production," *Fuel*, vol. 286, article 119447, 2021.

[36] B. Nath, B. Das, P. Kalita, and S. Basumatary, "Waste to value addition: utilization of waste *Brassica nigra* plant derived novel green heterogeneous base catalyst for effective synthesis of biodiesel," *Journal of Cleaner Production*, vol. 239, article 118112, 2019.

[37] R. Devasan, J. V. L. Ruatpuia, S. P. Gouda et al., "Microwave-assisted biodiesel production using bio-waste catalyst and process optimization using response surface methodology and kinetic study," *Scientific Reports*, vol. 13, no. 1, p. 2570, 2023.

[38] B. Nath, B. Basumatary, S. Brahma et al., "*Musa champa* peduncle waste-derived efficient catalyst: studies of biodiesel synthesis, reaction kinetics and thermodynamics," *Energy*, vol. 270, article 126976, 2023.

[39] O. A. Falowo and E. Betiku, "A novel heterogeneous catalyst synthesis from agrowastes mixture and application in transesterification of yellow oleander-rubber oil: optimization by Taguchi approach," *Fuel*, vol. 312, article 122999, 2022.

[40] O. A. Falowo, B. Oladipo, A. E. Taiwo, A. T. Olaiya, O. O. Oyekola, and E. Betiku, "Green heterogeneous base catalyst from ripe and unripe plantain peels mixture for the transesterification of waste cooking oil," *Chemical Engineering Journal Advances*, vol. 10, article 100293, 2022.

[41] B. Karmakar, A. Hossain, B. Jha, R. Sagar, and G. Halder, "Factorial optimization of biodiesel synthesis from castor-karanja oil blend with methanol-isopropanol mixture through acid/base doped *Delonix regia* heterogeneous catalysis," *Fuel*, vol. 285, article 119197, 2021.

[42] V. V. Vinu and N. N. Binitha, "Lithium silicate based catalysts prepared using arecanut husk ash for biodiesel production from used cooking oil," *Materials Today: Proceedings*, vol. 25, pp. 241–245, 2020.

[43] B. Basumatary, B. das, B. Nath, and S. Basumatary, "Synthesis and characterization of heterogeneous catalyst from sugarcane bagasse: production of jatropha seed oil methyl esters," *Current Research in Green and Sustainable Chemistry*, vol. 4, article 100082, 2021.

[44] N. Daimary, K. S. H. Eldiehy, P. Boruah, D. Deka, U. Bora, and B. K. Kakati, "Potato peels as a sustainable source for biochar, bio-oil and a green heterogeneous catalyst for biodiesel production," *Journal of Environmental Chemical Engineering*, vol. 10, no. 1, article 107108, 2022.

[45] G. P. Chutia, S. Chutia, P. Kalita, and K. Phukan, "*Xanthium strumarium* seed as a potential source of heterogeneous catalyst and non-edible oil for biodiesel production," *Biomass and Bioenergy*, vol. 172, article 106773, 2023.

[46] G. Kapildev, A. Chinnathambi, G. Sivanandhan et al., "High-efficient *agrobacterium*-mediated in planta transformation in black gram (*Vigna mungo* (L.) Hepper)," *Acta Physiologiae Plantarum*, vol. 38, no. 8, 2016.

[47] R. Saran, P. P. Sharma, and A. Dashora, "Correlation and path coefficient analysis for seed yield and its attributing traits in blackgram [*Vigna mungo* (L.) Hepper]," *Legume Research - An International Journal*, vol. 46, pp. 417–420, 2020.

[48] P. R. Narendrabhai and M. Bala, "Genetic divergence studies in black gram [*Vigna mungo* (L.) Hepper]," *International Journal of Chemical Studies*, vol. 8, no. 4, pp. 2777–2780, 2020.

[49] "Black gram Outlook," 2022, Retrieved on 25th June 2023. https://pjtsau.edu.in/files/AgriMkt/2022/Ocotber/blackgram-Ocotber-2022.pdf.

[50] S. Basumatary, B. Nath, B. Das, P. Kalita, and B. Basumatary, "Utilization of renewable and sustainable basic heterogeneous catalyst from *Heteropanax fragrans* (Kesseru) for effective synthesis of biodiesel from *Jatropha curcas* oil," *Fuel*, vol. 286, article 119357, 2021.

[51] P. Kodgire, A. Sharma, and S. S. Kachhwaha, "Optimization and kinetics of biodiesel production of *Ricinus communis* oil and used cottonseed cooking oil employing synchronised 'ultrasound + microwave' and heterogeneous CaO catalyst," *Renewable Energy*, vol. 212, pp. 320–332, 2023.

[52] M. A. Mujtaba, H. H. Masjuki, M. A. Kalam et al., "Ultrasound-assisted process optimization and tribological characteristics of biodiesel from palm-sesame oil via response surface methodology and extreme learning machine-cuckoo search," *Renewable Energy*, vol. 158, pp. 202–214, 2020.

[53] O. A. Falowo, T. V. Ojumu, O. Pereao, and E. Betiku, "Sustainable biodiesel synthesis from honne-rubber-neem oil blend with a novel mesoporous base catalyst synthesized from a mixture of three agrowastes," *Catalysts*, vol. 10, no. 2, p. 190, 2020.

[54] M. Aghbashlo, W. Peng, M. Tabatabaei et al., "Machine learning technology in biodiesel research: a review," *Progress in Energy and Combustion Science*, vol. 85, article 100904, 2021.

[55] J. Liu and B. Tao, "Fractionation of fatty acid methyl esters via urea inclusion and its application to improve the low-temperature performance of biodiesel," *Biofuel Research Journal*, vol. 9, no. 2, pp. 1617–1629, 2022.

[56] S. P. Yeong, Y. S. Chan, M. C. Law, and J. K. U. Ling, "Improving cold flow properties of palm fatty acid distillate biodiesel through vacuum distillation," *Journal of Bioresources and Bioproducts*, vol. 7, no. 1, pp. 43–51, 2022.

[57] B. Basumatary, S. Basumatary, B. Das, B. Nath, and P. Kalita, "Waste *Musa paradisiaca* plant: an efficient heterogeneous base catalyst for fast production of biodiesel," *Journal of Cleaner Production*, vol. 305, article 127089, 2021.

[58] T. F. Adepoju, B. E. Olatunbosun, O. M. Olatunji, and M. A. Ibeh, "Editorial Expression of Concern: Brette pearl spar Mable (BPSM): a potential recoverable catalyst as a renewable source of biodiesel from *Thevetia peruviana* seed oil for the benefit of sustainable development in West Africa," *Energy, Sustainability and Society*, vol. 11, no. 1, p. 17, 2021.

[59] S. Basumatary, P. Barua, and D. C. Deka, "Gmelina arborea and *Tabernaemontana divaricata* seed oils as non-edible feedstocks for biodiesel production," *International Journal of ChemTech Research*, vol. 6, pp. 1440–1445, 2014, http://sphinxsai.com/2014/CTVOL6/CT=70(1440-1445)AJ14.pdf.

[60] V. Vadery, B. N. Narayanan, R. M. Ramakrishnan et al., "Room temperature production of jatropha biodiesel over coconut husk ash," *Energy*, vol. 70, pp. 588–594, 2014.

[61] B. Nath, P. Kalita, B. das, and S. Basumatary, "Highly efficient renewable heterogeneous base catalyst derived from waste *Sesamum indicum* plant for synthesis of biodiesel," *Renewable Energy*, vol. 151, pp. 295–310, 2020.

[62] M. Gohain, A. Devi, and D. Deka, "*Musa balbisiana* Colla peel as highly effective renewable heterogeneous base catalyst for biodiesel production," *Industrial Crops and Products*, vol. 109, pp. 8–18, 2017.

[63] S. Niju, C. Anushya, and M. Balajii, "Process optimization for biodiesel production from *Moringa oleifera* oil using conch shells as heterogeneous catalyst," *Environmental Progress & Sustainable Energy*, vol. 38, no. 3, article e13015, 2019.

[64] R. S. Malani, V. Shinde, S. Ayachit, A. Goyal, and V. S. Moholkar, "Ultrasound–assisted biodiesel production using heterogeneous base catalyst and mixed non–edible oils," *Ultrasonics Sonochemistry*, vol. 52, pp. 232–243, 2019.

[65] W. Xie and X. Huang, "Synthesis of biodiesel from soybean oil using heterogeneous KF/ZnO catalyst," *Catalysis Letters*, vol. 107, no. 1-2, pp. 53–59, 2006.

[66] T. F. Adepoju, "Optimization processes of biodiesel production from pig and neem (*Azadirachta indica* a. Juss) seeds blend oil using alternative catalysts from waste biomass," *Industrial Crops and Products*, vol. 149, article 112334, 2020.

[67] T. F. Adepoju, "Synthesis of biodiesel from *Annona muricata–Calophyllum inophyllum* oil blends using calcined waste wood ash as a heterogeneous base catalyst," *MethodsX*, vol. 8, p. 101188, 2021.

[68] T. F. Adepoju, M. A. Ibeh, E. O. Babatunde, and A. J. Asquo, "Methanolysis of CaO based catalyst derived from egg shell-snail shell-wood ash mixed for fatty acid methylester (FAME) synthesis from a ternary mixture of *Irvingia gabonensis-Pentaclethra macrophylla-Elais guineensis* oil blend: an application of simplex lattice and central composite design optimization," *Fuel*, vol. 275, article 117997, 2020.

[69] M. Gohain, K. Laskar, A. K. Paul et al., "*Carica papaya* stem: a source of versatile heterogeneous catalyst for biodiesel production and C–C bond formation," *Renewable Energy*, vol. 147, pp. 541–555, 2020.

[70] M. Sharma, A. A. Khan, S. K. Puri, and D. K. Tuli, "Wood ash as a potential heterogeneous catalyst for biodiesel synthesis," *Biomass and Bioenergy*, vol. 41, pp. 94–106, 2012.

[71] C. Li, X. Hu, W. Feng, B. Wu, and K. Wu, "A supported solid base catalyst synthesized from green biomass ash for biodiesel production," *Energy Sources, Part A: Recovery, Utilization, and Environmental Effects*, vol. 40, no. 2, pp. 142–147, 2018.

[72] B. Changmai, P. Sudarsanam, and S. L. Rokhum, "Biodiesel production using a renewable mesoporous solid catalyst," *Industrial Crops and Products*, vol. 145, article 111911, 2020.

[73] B. Basumatary, S. Brahma, B. Nath, S. F. Basumatary, B. Das, and S. Basumatary, "Post-harvest waste to value-added materials: *Musa champa* plant as renewable and highly effective base catalyst for Jatropha curcas oil-based biodiesel production," *Bioresource Technology Reports*, vol. 21, article 101338, 2023.

[74] K. J. Tamuli, R. K. Sahoo, and M. Bordoloi, "Biocatalytic green alternative to existing hazardous reaction media: synthesis of chalcone and flavone derivativesviathe Claisen–Schmidt reaction at room temperature," *New Journal of Chemistry*, vol. 44, no. 48, pp. 20956–20965, 2020.

[75] I. M. Mendonça, O. A. R. L. Paes, P. J. S. Maia et al., "New heterogeneous catalyst for biodiesel production from waste tucumã peels (*Astrocaryum aculeatum* Meyer): parameters optimization study," *Results in Engineering*, vol. 130, pp. 103–110, 2019.

[76] S. de S Barros, W. A. G. Pessoa Junior, I. S. C. Sá et al., "Pineapple (*Ananás comosus*) leaves ash as a solid base catalyst for biodiesel synthesis," *Bioresource Technology*, vol. 312, p. 123569, 2020.

[77] P. Prajapati, S. Shrivastava, V. Sharma et al., "Karanja seed shell ash: a sustainable green heterogeneous catalyst for biodiesel production," *Results in Engineering*, vol. 18, article 101063, 2023.

[78] J. B. Tarigan, K. Singh, J. S. Sinuraya et al., "Waste passion fruit peel as a heterogeneous catalyst for room-temperature biodiesel production," *ACS Omega*, vol. 7, no. 9, pp. 7885–7892, 2022.

[79] M. Farooq, A. Ramli, and A. Naeem, "Biodiesel production from low FFA waste cooking oil using heterogeneous catalyst derived from chicken bones," *Renewable Energy*, vol. 76, pp. 362–368, 2015.

[80] M. Farooq, A. Ramli, A. Naeem et al., "Biodiesel production from date seed oil (*Phoenix dactylifera* L.) via egg shell derived heterogeneous catalyst," *Chemical Engineering Research and Design*, vol. 132, pp. 644–651, 2018.

[81] A. O. Etim, P. Musonge, and A. C. Eloka-Eboka, "A green process synthesis of bio-composite heterogeneous catalyst

for the transesterification of linseed-marula bi-oil methyl ester," *Results in Engineering*, vol. 16, article 100645, 2022.

[82] E. K. L. Mares, M. A. Gonçalves, P. T. S. da Luz, G. N. da Rocha Filho, J. R. Zamian, and L. R. V. da Conceição, "Acai seed ash as a novel basic heterogeneous catalyst for biodiesel synthesis: optimization of the biodiesel production process," *Fuel*, vol. 299, article 120887, 2021.

[83] I. M. Mendonça, F. L. Machado, C. C. Silva et al., "Application of calcined waste cupuaçu (*Theobroma grandiflorum*) seeds as a low-cost solid catalyst in soybean oil ethanolysis: statistical optimization," *Energy Conversion and Management*, vol. 200, article 112095, 2019.

[84] D. T. Bekele, N. T. Shibeshi, and A. S. Reshad, "KNO_3-loaded coffee husk ash as a heterogeneous alkali catalyst for waste frying oil valorization into biodiesel," *ACS Omega*, vol. 7, no. 49, pp. 45129–45143, 2022.

[85] S. E. Mahesh, A. Ramanathan, K. M. M. S. Begum, and A. Narayanan, "Biodiesel production from waste cooking oil using KBr impregnated CaO as catalyst," *Energy Conversion and Management*, vol. 91, pp. 442–450, 2015.

[86] A. S. Yusuff, A. K. Bhonsle, J. Trivedi, D. P. Bangwal, L. P. Singh, and N. Atray, "Synthesis and characterization of coal fly ash supported zinc oxide catalyst for biodiesel production using used cooking oil as feed," *Renewable Energy*, vol. 170, pp. 302–314, 2021.

[87] N. Bhuyan, R. Narzari, L. Gogoi et al., "Valorization of agricultural wastes for multidimensional use," in *Current Developments in Biotechnology and Bioengineering*, pp. 41–78, Elsevier, 2020.

[88] T. F. Adepoju, M. A. Ibeh, E. N. Udoetuk, and E. O. Babatunde, "Quaternary blend of *Carica papaya-Citrus sinesis-Hibiscus sabdariffa*-waste used oil for biodiesel synthesis using CaO-based catalyst derived from binary mix of *Lattorina littorea* and *Mactra coralline* shell," *Renewable Energy*, vol. 171, pp. 22–33, 2021.

[89] H. C. Ong, J. Milano, A. S. Silitonga et al., "Biodiesel production from *Calophyllum inophyllum-Ceiba pentandra* oil mixture: optimization and characterization," *Journal of Cleaner Production*, vol. 219, pp. 183–198, 2019.

[90] A. S. Vinayaka, B. Mahanty, E. R. Rene, and S. K. Behera, "Biodiesel Production by Transesterification of a Mixture of Pongamia and Neem Oils," *Biofuels*, vol. 12, no. 2, pp. 187–195, 2018.

[91] A. B. Fadhil, E. T. B. Al-Tikrity, and M. A. Albadree, "Biodiesel production from mixed non-edible oils, castor seed oil and waste fish oil," *Fuel*, vol. 210, pp. 721–728, 2017.

[92] E. M. Vargas, L. Ospina, M. C. Neves, L. A. C. Tarelho, and M. I. Nunes, "Optimization of FAME production from blends of waste cooking oil and refined palm oil using biomass fly ash as a catalyst," *Renewable Energy*, vol. 163, pp. 1637–1647, 2021.

[93] A. N. Amenaghawon, M. O. Omede, G. O. Ogbebor et al., "Optimized biodiesel synthesis from an optimally formulated ternary feedstock blend via machine learning-informed methanolysis using a composite biobased catalyst," *Bioresource Technology Reports*, vol. 25, article 101805, 2024.

[94] Y. Zou, S. Tang, S. Tamjidi, B. K. Moghadas, and H. Esmaeili, "Ultrasound irradiation-assisted biodiesel synthesis from waste oils employing a retrievable and strong $CoFe_2O_4$/GO/SrO nanocatalyst," *Fuel*, vol. 361, article 130775, 2024.

[95] J. L. Aleman-Ramirez, P. U. Okoye, U. Pal, and P. J. Sebastian, "Agro-industrial residue of *Pouteria sapota* peels as a green heterogeneous catalyst to produce biodiesel from soybean and sunflower oils," *Renewable Energy*, vol. 224, article 120163, 2024.

[96] A. Sarkar, P. Das, I. B. Laskar, S. Vadivel, A. Puzari, and B. Paul, "*Parkia speciosa*: a basic heterogeneous catalyst for production of soybean oil-based biodiesel," *Fuel*, vol. 348, article 128537, 2023.

[97] J. L. Aleman-Ramirez, P. U. Okoye, S. Torres-Arellano et al., "Development of reusable composite eggshell-moringa leaf catalyst for biodiesel production," *Fuel*, vol. 324, article 124601, 2022.

[98] J. Yang, W. J. Cong, Z. Zhu et al., "Microwave-assisted one-step production of biodiesel from waste cooking oil by magnetic bifunctional SrO–ZnO/MOF catalyst," *Journal of Cleaner Production*, vol. 395, article 136182, 2023.

[99] E. K. Sitepu, R. P. A. Sinaga, B. E. N. Sitepu et al., "Calcined biowaste durian peel as a heterogeneous catalyst for room-temperature biodiesel production using a homogenizer device," *ACS Omega*, vol. 9, no. 13, pp. 15232–15238, 2024.

[100] M. Saad, B. Siyo, and H. Alrakkad, "Preparation and characterization of biodiesel from waste cooking oils using heterogeneous catalyst (Cat. TS-7) based on natural zeolite," *Heliyon*, vol. 9, no. 6, article e15836, 2023.

[101] P. J. Ahranjani, S. F. Saei, G. A. El-Hiti, K. K. Yadav, J. Cho, and S. Rezania, "Magnetic carbon nanotubes doped cadmium oxide as heterogeneous catalyst for biodiesel from waste cooking oil," *Chemical Engineering Research and Design*, vol. 201, pp. 176–184, 2024.

[102] I. Fatimah, D. Rubiyanto, A. Taushiyah, F. B. Najah, U. Azmi, and Y. L. Sim, "Use of ZrO_2 supported on bamboo leaf ash as a heterogeneous catalyst in microwave-assisted biodiesel conversion," *Sustainable Chemistry and Pharmacy*, vol. 12, article 100129, 2019.